

The paper title was changed to “Net ecosystem exchange and energy fluxes measured with eddy covariance technique in a West Siberian bog”. We think the new version better underlines the novelty of the study.

5 **Response to Review #1**

C. Wille (Referee)

christian.wille@gfz-potsdam.de

10 Received and published: 13 March 2017

General Comments

15 The manuscript presents energy and CO₂ flux data from the West Siberian Taiga. This is valuable data, as the West Siberian Lowland is a vast understudied region. The presented 4-month data set is the first data of what is to become a permanent flux measurement site. Thus it can provide a base line for comparison with other sites and with data that will be collected at the same site in the years ahead.

20 Generally, the style of the manuscript and the presentation of data is adequate. However, the data analyses lag behind the state of the art and the discussion of the results is often weak. Extensive revisions are necessary before publication of the manuscript.

[We express our gratitude for the time invested in deep analysis of our manuscript and for the many useful comments that have resulted from it.](#)

25

Main Critique

30 (1) No information on the gap-filling of energy fluxes is given. Was gap-filling not performed for H and LE? Monthly means of these values could be seriously biased if they are calculated based on non-gap-filled time series. Gap-filling should be performed in order to derive sound estimates of mean or cumulative fluxes, and the methods used should be clearly presented in the methods section.

35 [You are correct, the original non-gapfilled energy fluxes were presented in the original MS draft, as we considered that the data series were complete enough \(at least in May-July\) for the means not to be biased. However, we understand the concern and have done gapfilling of the energy fluxes. Soil heat flux is calculated from gapfilled soil temperature and water level data, therefore, it's gap-free. The other fluxes are gapfilled according to the accepted routines, e.g. Falge et al. \(2001\). The more in-depth explanation can be found in the revised manuscript \(section 2.5\). However, the changes after gapfilling, in terms of average or cumulative values \(including Bowen ratio\) were small.](#)

40

45 (2) How have the authors addressed the heterogeneity of soil and hydrological properties and hence ground heat flux (G)? Was soil temperature measured and G calculated for only one microform, hummock or hollow? As G could be expected to vary strongly between hummocks and hollows, a weighted average (based on surface area fractions) of G calculated for both microforms should be used. If G is available for only one microform, an estimate of the error induced by this approach should be added (which could also serve as a justification for this approach).

50 The originally presented soil heat flux was calculated for hollows, as they are the dominating
microform within the EC footprint. To account for this comment in the revision, we calculate G as
an area-weighted average for hummocks and hollows (using two replicates of temperature profile in
each microform). At the same time, the hydrological differences are tackled by using the ridge and
hollow water level measurements in the calculation of the corresponding heat fluxes.

55 (3) In my opinion, an instationarity test (e.g. Foken and Wichura, 1996) is start of the
art and should be applied.

We have applied the instationarity test in the new version of the manuscript and it did not introduce
a statistically significant change in the observed fluxes, because it mainly remove very small fluxes
(those close to zero). For instance, only a fraction of the negative nocturnal CO₂ flux values were
removed by this filter. However, it appears that the new method of Re and GPP model parameter
60 estimation is robust enough so that non-stationarity filtering can be implemented without significant
increase in parameter uncertainty. This is done in the revision with a non-stationarity threshold of 1.

(4) No information on the seasonal vegetation development is given in the manuscript.
Even if assessments/measurements of GAI or LAI are not available, a general description
65 of the vegetation development is indispensable in order to put the observed flux
data in context to the annual cycle of fluxes and drivers.

1)_ Unfortunately, no LAI or snow monitoring has been done during the study period. Therefore,
only approximate qualitative estimation of the two parameters can be offered.

70 Additionally, as the measurements started directly after the end of snow melt, information on the
snow/soil conditions immediately before the beginning of the measurement period should be added,
if possible (snow height, snow water equivalent, beginning of snow melt, depth of frozen peat layer,
beginning/end of peat thaw). This could be very helpful to understand the temporal development of
fluxes at the beginning of the growing season.

75 2) The snowmelt is shown by the steep downward trend in PAR albedo, indicating the presence of
patches of snow until about 3 May. However, all profiles, except one in the hollow, indicate
freezing at -5 cm until 3rd May, and until about 6th May at -20 cm. Therefore, the snowmelt and peat
thaw proceeded only over the first few days of the study. The quantities such as snow pack depth or
snow water equivalent are, unfortunately, currently unavailable.

80 (5) The partitioning of measured net ecosystem exchange (NEE), particularly the modelling
of ecosystem respiration (Re) appears to be not sound. In Detail: (a) Why are
there significant negative fluxes in the Re vs. peat temperature (Tp) plot (Fig. 3a)?

85 After careful QA/QC I would ideally expect to see only few and small negative night
time CO₂ fluxes (predominantly at lower temperatures). Maybe, the application of an
instationarity test could help removing these conspicuous data points? (b) The fit of
eq. 6 to the Re vs. Tp data set (Fig. 3a) seems to have a low R². I'd like to see the
R² and p values for this fit. (d) Generally, combining data from the period May-August
90 in one fit of Re vs. Tp is likely to confound the seasonal development of Rref with its
temperature dependence. This is reflected in the large temperature sensitivity (Q10
value) obtained by the fit. Fitting Re vs. Tp in a moving window of length 10: :30 days
would be more appropriate. If this would lead to unrealistic variations of the reference
respiration (Rref) and Q10, the authors could constrain Q10 to a value around 1.5 (cf.
Mahecha et al., 2010). This way, at least the variation of Rref could be assessed, which
95 could give valuable insights into the seasonal vegetation development.

We faced challenges with energy supply at the Mukhrino station. With many cloudy and low-wind
periods, frequent blackouts occurred, especially in the nighttime periods. Eventually, this led to the

100 nocturnal data being scarce as it is. The existing nighttime data were only sufficient to construct one general fit of R_e vs. T_p (Fig. 3a). Therefore, unfortunately, recalculation of both R_e model parameters (R_{e_ref} and Q_{10}) in a moving window does not seem possible. However, a different modeling/partitioning method was used instead. It offers a tradeoff between robustness, precision and the ability to resolve the seasonal course of the parameters, incorporating the following steps:

The updated modeling/gapfilling approach

105 a) The complete NEE equation, $NEE = R_{ref} * Q_{10}^{(T_{moss}-12)/10} - (P_{max} * PAR)/(k+PAR)$, is fit to the data at $PAR < 300 \text{ W/m}^2$, in the region where exchange is dominated by respiration. This fit yields $Q_{10} = 1.99$, 95% CI [1.42; 2.57]. This value of Q_{10} is fixed for the entire May-August period. Regarding the Reviewer's remark on Q_{10} , we would in return suggest that it mainly stems from the choice of the driving temperature, and, as such, does not carry much biological meaning.

110 b) The R_{ref} , P_{max} and k parameters are evaluated in a 30-day wide moving time window.

c) The R_{ref} , P_{max} and k series are spline-interpolated to produce the 30-min series, after which the models can be calculated at the original data resolution.

The overview of the gapfilling method is included in the revision (section 2.6).

115 The superior performance of the described method, compared with its older version, is revealed by a smaller model-measured intercept (see e.g. the figure with the mean diurnal CO_2 flux course).

Flux nonstationarity filtering.

120 Filtering the CO_2 flux for high nonstationarity does remove a number of nighttime data in addition to the u^* filter; however, the data points so excluded are randomly distributed over the entire nighttime R_e range (i.e. both negative and positive values are affected). The negative values in nocturnal F_{CO_2} likely result from high random uncertainty, i.e. they are counterweighted by similarly high positive values. In the revised version of the manuscript, the FST filter is used with the threshold of 1.

125 To sum it up, we believe that the mean flux-temperature regression, in both its old and new versions, is realistic. This is supported by the fact that the general R_e model of Mukhrino does look similar to those found in the other sites. For example, in a similar Siikaneva-2 site (Southern Finnish bog), an ensemble of data from 4 growing seasons showed $R_{ref} = 0.8 \mu\text{mol m}^{-2} \text{ s}^{-1}$ and $Q_{10} = 3.5$.

130

Specific Comments

135 Line 123: On which micro-form was soil temperature measured (hummock/hollow)?
See (2) in Section "Main Critique" above.

The presented soil temperature and the derived heat flux were measured at a hollow microform. However, in the revision we use a total of four profiles, in hollow and ridge. The area-weighted average ridge-hollow temperature time series are shown in Fig. 4a.

140

Line 169: For which micro-form was ground heat flux calculated (hummock/hollow)?
See (2) in Section "Main Critique" above.

In the original MS version, at the hollow microform. However, the difference between the updated and old G is not great, in correspondence with the dominance of hollows.

145

Lines 193-194: Why was only CO_2 night time data of August excluded from analysis?
It is hard to imagine that only CO_2 fluxes are compromised by technical problems of

the gas analyzer but not LE fluxes.

150 The source of the problem affecting the August nocturnal CO₂ flux is not known. The R_{ref} parameter increases notably in August, and it is difficult to say if this is a natural dynamic or a technical problem. The objective quality criteria do not remove those data. However, LE seems not to be affected, as its August nighttime values are close to zero as in the previous months. In any case, we decided to keep the August data, but be tentative in its interpretation.

155

Lines 205-206: Why was night-time defined as periods with a solar elevation angle below 5° and not by a PAR threshold (e.g. PAR < 20 μmol/m²/s)? Using a local PAR threshold may allow additional data points to be included into the night time data set (e.g. during cloudy conditions), which could improve the data coverage and hence the modelling of R_e.

160

The night definition was updated as proposed, as the periods with PAR < 10 μmol m⁻² s⁻¹.

Line 206: Have you tried to use peat temperature from other depths or air temperature for the modelling of R_e? Information on the performance of the model with other temperatures could give valuable insights into the source of respired CO₂.

165

Yes, we did try to use the other temperatures as drivers of respiration. The hummock temperature measurement had been previously used for that purpose. This is consistent with much higher density of vegetation and low water level in hummocks, which probably makes them major contributors to ecosystem respiration despite representing a smaller area fraction than hollows.

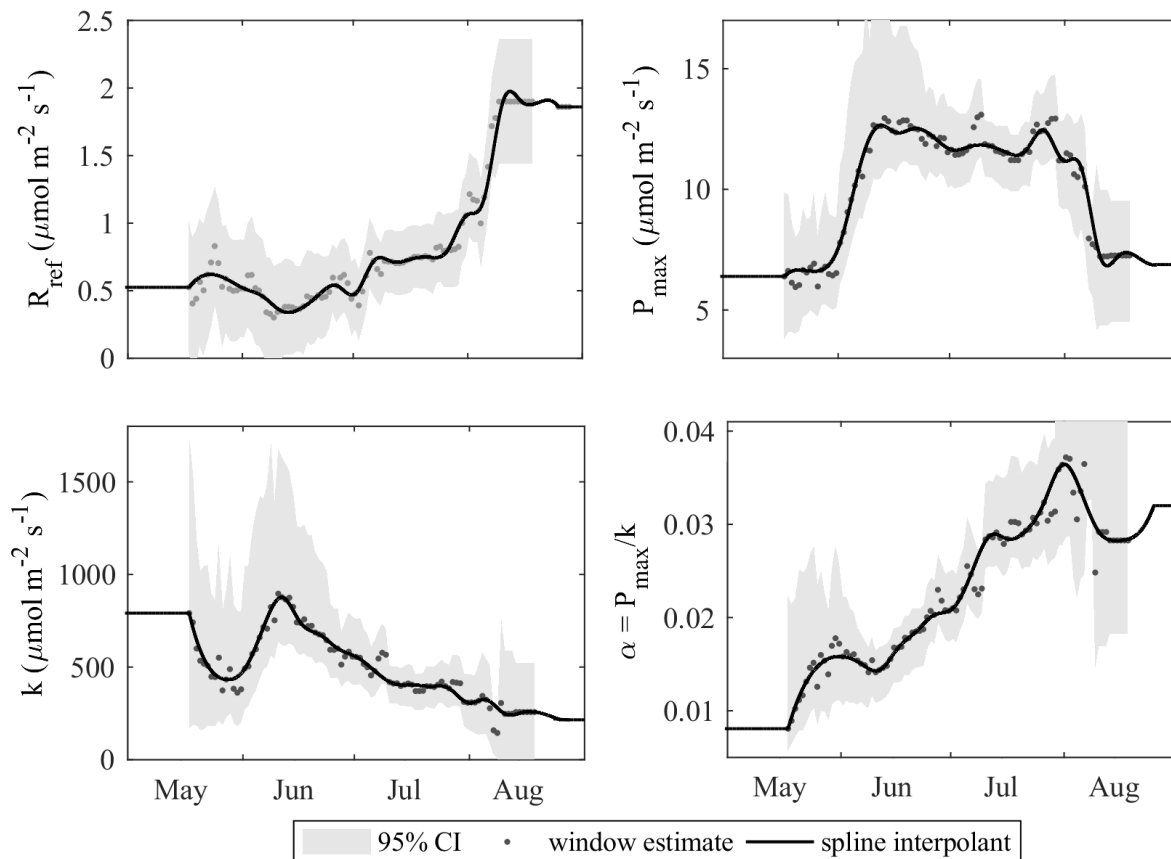
170

However, in consistency with the revised soil heat flux, we are now using the area-weighted soil surface temperature also in R_e modeling.

Lines 219-221: In which time steps was the 30-day window moved? Please add this information. Further, the time series of the fit parameters P_{max} and k (or the often used alpha = P_{max}/k) should be presented. This could deliver valuable information on the seasonal development of the vegetation and could be compared to other studies.

175

The time window was moved in 1 day steps. We will present the P_{max}, k and alpha parameter timeseries in a new figure or subplot. Please also see the requested data in Fig. R1 below.



180

Figure R1. The timeseries of the CO₂ flux model parameters. The dots are the daily values estimated in a moving window 30 days wide; the solid lines are the spline interpolants, and the shaded area is the 95% confidence interval (calculated in each time window). This figure will be included in the revised manuscript.

185

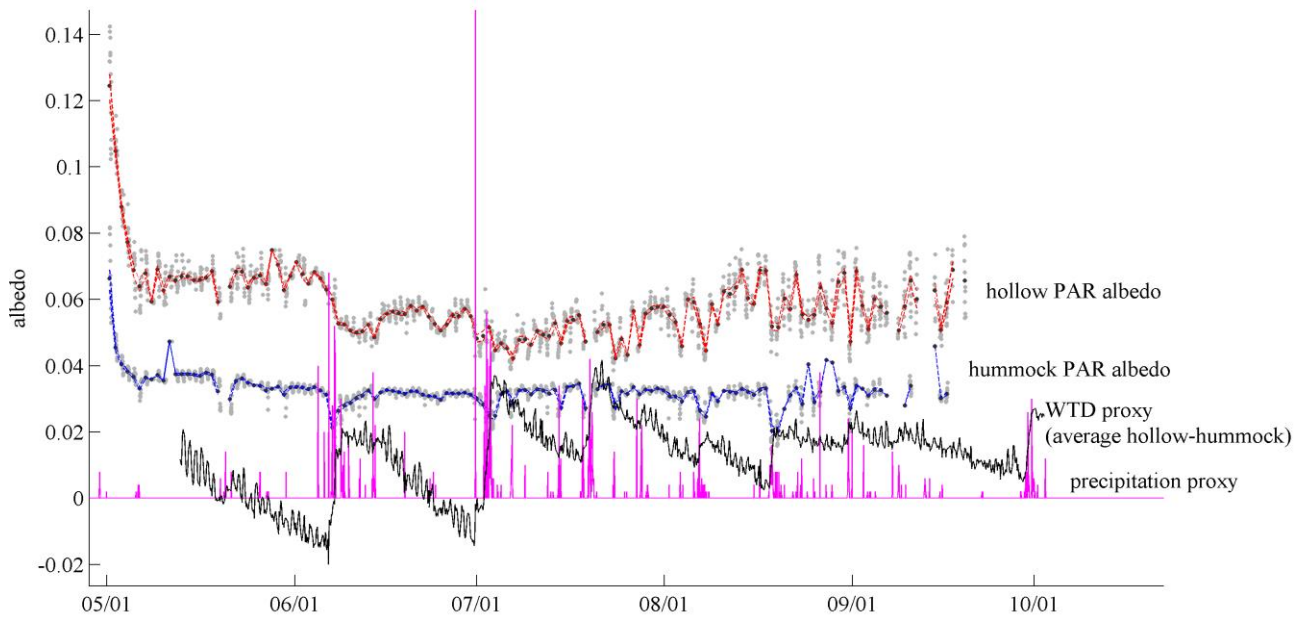
Lines 234-236: Soil temperature at depths 20 cm and 50 cm is discussed here, but this data is neither displayed in Fig. 4a nor used in the analyses. I suggest to either add this data in an additional subplot of Fig. 4 or concentrate in the text on the data already displayed in Fig. 4, i.e. T_p at 5 cm depth.

190

This mismatch between the text and the plots in Fig.4 is confusing indeed. We will add the 20 and 50 cm temperatures in the subplot (a) of Fig.4.

195

Lines 258-259: The statement “: : later on during the summer the water level decreases: :” contradicts what is shown in Fig. 4e, and is stated in lines 344-345, “The regular and ample precipitation helped sustain water level at a nearly constant level: :”. Hence, the authors’ assumption that albedo is reduced due to drying of the vegetation is ill-conceived. Still, it could be checked by simply calculating an albedo from incoming and reflected PAR.



200

Figure R2. PAR albedo for the hollow and hummock microforms calculated as diurnal medians of the midday (10AM-16PM) periods. The grey dots are the original 30-min albedo averages. WTD (black) and precipitation (purple) proxies are also shown for reference.

205

Our original expectation was to see an increase in albedo during the dry spells (lines 258-259), which is commonly observed in other peatlands worldwide. However, the year 2015 being unusually wet, the water table did not follow its typical downward trend, nor did dry spells last long. In fact, there were at least seven periods of WTD drawdown and subsequent recovery during heavy rainfalls. On average, WTD had maybe remained constant throughout the growing season. The time-series of albedo are shown in Fig.R2 above. Albedo was rather stable at about 0.06 in hollow and 0.04 in hummock, although small variation correlated with WTD and precipitation can be seen. Similar peatland PAR albedo values were found in other studies (e.g. 5.5% in Frolking et al. 1998). In general, the correlation with rainfall seems to be higher than that with WTD, which is consistent with the expectation that surface wetness is a stronger controller than WTD. WTD may be decoupled from surface wetness, which is especially probable in hummock, meaning that WTD is probably an inferior predictor of surface wetness and, hence, albedo. In this sequence of frequent rewetting events and drying periods, the surface wetness and albedo shows simultaneous peaks, which is illustrated well by the hummock measurements (Fig. R2).

210

215

Of course, the phenology (course of LAI, etc.) in sedge in other vascular species must have affected albedo in a way that is difficult to estimate for the lack of observations. Qualitatively, the dark-colored living vascular plant biomass should lower the ecosystem albedo around the peak of the growing season.

220

Also, note the steep albedo plunge in early May, indicative of the final snowmelt stage.

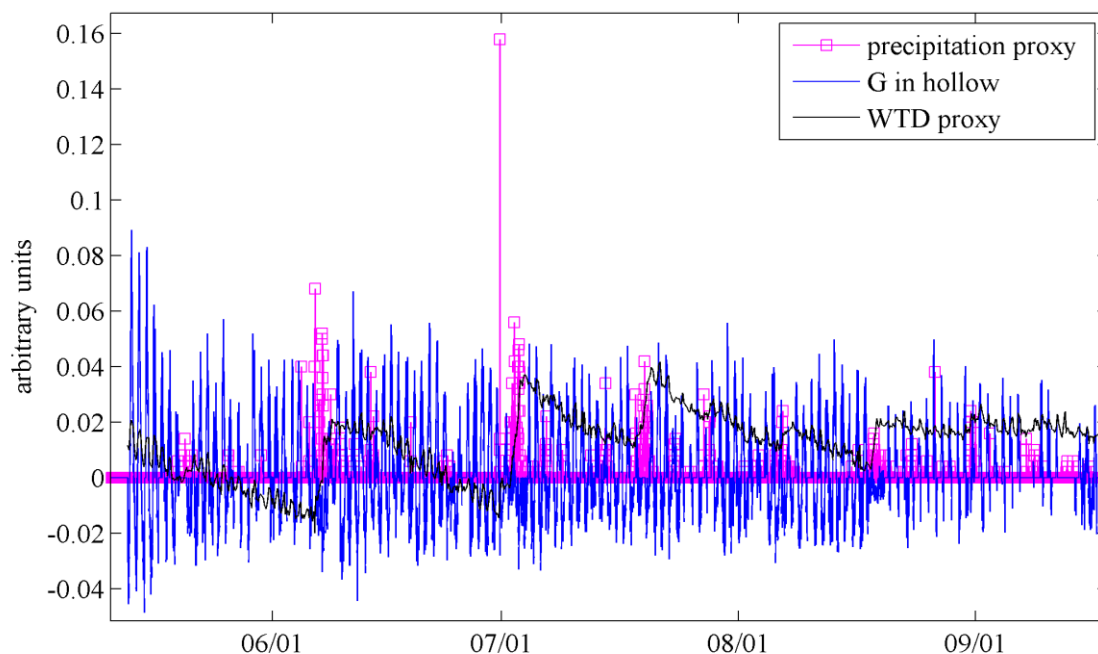
225

Line 302: The spatial heterogeneity does not seem to serve as a good explanation for the low value of the energy balance closure in May, as the surface heterogeneity does not change during the course of the measurement period. Or does it change? How?

230

The change in the area of open water pools is mentioned as one of the possible sources of heterogeneity in May (line 302), which, in turn, may affect the ground heat flux (line 303). This was the month when the snowmelt ended, which is typically accompanied by scattered open water pools. Their locations were not recorded. We do not know how the surface energy balance

235 measurements could have been affected by those spring conditions. The ground heat flux in hollow was very variable during May, reaching the highest levels for the whole growing season in mid-May with a subsequent reduction to the average annual levels (Fig. R3), suggesting some rapid changes in the thermal properties of the ground.



240 Figure R3. Timeseries of the ground heat flux in hollow, precipitation and WTD. The units are arbitrary.

Line 310 and Fig. 8a caption: The data displayed is surely modelled NEE and not measured NEE?

245 We apologize for the inconsistency - this is actually gapfilled NEE, i.e. the quality-controlled and u^* -filtered original NEE record with the gaps filled by the NEE model.

Lines 311-312: Could the lower amplitude of NEE in May also be due to a not fully developed foliage of the vegetation? Snow melt had only ended a few days before and below-zero temperatures still seem to occur during May. Time series of the parameters P_{max} , k , and R_{ref} could help to explain the variations in observed NEE.

250 You are absolutely right. The ground vascular vegetation (shrubs, sedges) would have only started to recover from the winter and grow their leaf area. While R_{ref} cannot be resolved on a finer timescale for the reasons discussed above. Exactly as suggested, P_{max} shows a steep upward trend between May and June, the period of green biomass accumulation. The time-series of the model parameters are now shown in a Figure 3 in the revised manuscript.

260 Lines 213-314: I see a systematic difference of measured and modelled NEE in Fig. 9. In the afternoon hours of July, measured NEE uptake is smaller than modelled NEE uptake. Hence, either R_e is underestimated or GPP is overestimated. What could be the reason for this? Furthermore, why is August night time CO_2 flux data displayed if it should have been excluded from analysis due to technical problems (line 194)? In fact, this data does not look completely unrealistic to me. Gažovič et al. (2013) has observed the highest R_e during August, while GPP peaked in July. The discrepancies between modelled and measured fluxes could be caused by the fact that R_e is poorly

265 modelled by the approach chosen by the authors.
The general observation relating to the new modeling results is that this mismatch is mainly gone. It seems that, just as you have suggested, the model-measured NEE mismatch had been caused by the suboptimal Re modelling method and/or the choice of the driving temperature. In any case, the updated version of the NEE model is probably good enough for the gapfilling purposes.
270 We also agree (as in the response to an earlier comment) that the August respiration data might be correct. The hypothesis about the technical problems in August has not been confirmed after a cross-check; it was established during revision that no objective filtering or quality control steps could remove the August data. It is also encouraging to hear that some studies, including Gažovic et al. (2013), found similar seasonal trends, thank you for pointing this out. However, data coverage in
275 August is still very low, and the results from that month should be treated with caution.

Lines 352-353 and Fig. 10: Combining all data from the period May-August potentially confounds the seasonal development of Pmax and k, and hence GPPmod, with a possible short term variation of these parameters due to their temperature dependence.
280 For this approach, only data from the peak vegetation period, i.e. June and July, should be used. Ideally, also the window length for the fit of eq. 7 and determination of parameters Pmax and k should be reduced.
We understand the logic behind this comment. However, as the GPP model used for normalization was calculated from the seasonally changing Pmax and k series, it thus implicitly includes LAI development and other low-frequency seasonal factors, although short-term variability may be lost.
285 We have experimented with different time windows of Pmax and k, and found that at lengths shorter than 1 month, the random variability increasingly dominated the real signal. This was due to the gaps in the original 30-min data, which can only be circumvented by using a sufficiently wide time window. Nevertheless, since May represents the spring recovery period, and August is not
290 covered with data well, using only June and July would improve this analysis. However, for June-July, the picture remains about the same (Fig. R4). Reducing the window length to under 1 month is problematic, due to the scarcity of the nighttime data, but we believe that the current length allows evaluating the seasonal change, at the least.
The observed NEE normalized with the NEE model vs. air temperature for June-July 2015 can now
295 be seen in Fig. 10b of the revised manuscript.

Technical Corrections

Line 66: Use same units as in line 64, i.e. km².
300 Done

Line 72: Is there Permafrost at all at this site, i.e. discontinuous Permafrost? Please clarify.
There is no permafrost of any type in Mukhrino or anywhere else in the region; this is clarified in
305 the revision.

Line 302: Replace “somehow” with “to some extent”.
Done

Line 367: “GPP normalized by its model” is ambiguous. Use “(NEE - Rmod)/GPPmod”.
Done

References

315

Foken T, Wichura B (1996): Tools for quality assessment of surface-based flux measurements. *Agricultural and Forest Meteorology*, 78, pp. 83-105. DOI:10.1016/0168-1923(95)02248-1.

320

Gažovič et al. (2013): Hydrology-driven ecosystem respiration determines the carbon balance of a boreal peatland. *Science of the Total Environment*, 463-464, pp. 675–682. Mahecha et al. (2010): Global Convergence in the Temperature Sensitivity of Respiration at Ecosystem Level. *Science*, Vol. 329, Issue 5993, pp. 838-840. DOI: 10.1126/science.1189587.

325

Frolking, S.E., Bubier, J.L., Moore, T.R., Ball, T., Bellisario, L.M., Bhardwaj, A., Carroll, P., Crill, P.M., Lafleur, P.M., McCaughey, J.H., Roulet, N.T., Suyker, A.E., Verma, S.B., Waddington, J.M. and Whiting, G.J. (1998). Relationship between ecosystem productivity and photosynthetically active radiation for northern peatlands. *Global Biogeochemical Cycles* 12: doi: 10.1029/97GB03367.

330

Falge, E., Baldocchi, D., Olson, R., Anthoni, P., Aubinet, M., Bernhofer, C., Burba, G., Ceulemans, R., Clement, R., Dolman, H., Granier, A., Gross, P., Grunwald, T., Hollinger, D., Jensen, N.O., Katul, G., Keronen, P., Kowalski, A., Lai, C.T., Law, B.E., Meyers, T., Moncrieff, J., Moors, E., Munger, J.W., Pilegaard, K., Rannik, U., Rebmann, C., Suyker, A., Tenhunen, J., Tu, K., Verma, S., Vesala, T., Wilson, K., Wofsy, S., 2001. Gap filling strategies for defensible annual sums of net ecosystem exchange. *Agric. Forest Meteorol.* 107, 43–69.

335

340

Response to Review #2

345

Anonymous Referee #2

Received and published: 3 April 2017

350

The manuscript presents net ecosystem and energy fluxes from a West Siberian bog measured by eddy covariance technique. This manuscript provides important data from a remote and large but also understudied region which is characterized by high coverage of peatlands. Unfortunately, the data presented here is just for 4 summer months but as it was measured at an established field station more data will surely follow in the future. The topic of the manuscript is well within the scope of the journal

355

and the manuscript meets well the basic scientific quality. However, extensive revisions are necessary before publication of manuscript.

Dear reviewer, we express our gratitude for your detailed analysis of the current manuscript. We will try to address all the comments.

360 **Main points of critique**

1. It would be important to include some information on vegetation development over the investigated period to better understand the dynamic of the CO₂ fluxes.

365 Unfortunately, the vegetation parameters (such as LAI, biomass or phenology) were not directly assessed during the course of the measurements. Therefore, we can only offer qualitative estimates.

2. The gap filling procedures should be described in more detail. It should be clarified in the text and in the figures if modelled or measured data has been used and also discussed how the gap filling method might influence the modelled data. If gap filling was not applied it should be discussed which influence it would have on the results.

370 This is correct, the CO₂ flux data series have been gapfilled already in the original MS, and both the gapfilled and non-gapfilled series were displayed throughout the manuscript, depending on the aims of the individual sections. We will specify this more clearly in the text and explain the gapfilling procedure in more detail. The modeling/gapfilling method has also been revised; please see the detailed explanation in the answer to a comment by Reviewer 1. Please see the revised MS sections 375 2.5 and 2.6 for the description of the updated gapfilling procedures for the energy and CO₂ fluxes.

3. The discussion is weak, maybe that was the reason why results and discussion were merged in one chapter. This chapter includes mainly comparison to other studies and less discussion of the influencing factors which determine the dynamics of CO₂ and heat fluxes.

380 We understand this comment and will try to improve the discussion. We will revise the discussion of the environmental driver effects as much as it is possible with the available dataset, as much as the available data permits.

385 **Specific comments:**

L 38: Please include some examples for measurements in Europe and in Siberia.

390 We will mention the relevant examples of bog measurements in the region. However, very few other peatland studies have been conducted in the region – this not only including West-Siberian middle taiga, but in Siberia as a whole. The number of relevant studies becomes even more limited if one considers only raised bog ecosystems. The revised MS lines 39-44 now list the comparable sites having eddy-covariance setups.

395

L 55 Please change to flux tower data

Thank you for noticing this slip of the pen, this will be corrected.

L 114 I usually include the measurement section into the methods section

400 It will maybe make more sense indeed to combine the ‘Materials’ and ‘Methods’ sections; this is done in the revised version.

L128-130 You do not present winter fluxes here, so you can skip that paragraph or when does the winter start?

405 This is in fact the first description of the measurement site and its infrastructures that has not appeared in any prior English language publications. We therefore tried to include all the information that could potentially be of interest. In fact, in 2015 the snowmelt ended in the very

beginning of May, as suggested by the PAR albedo timeseries (Fig. R2 in the response to Reviewer 1).

410

L205 Why do you use the solar elevation angle and not the widely used $\text{PAR} < 10 \text{ } \mu\text{mol}/\text{m}^2\text{s}$ threshold to define the night-time?

415

The solar elevation angle criterion has also been widely used in our community. A possible issue with using the PAR threshold is that PAR is measured at about 2m height, while the eddy-covariance sensors are installed at 4m height. Furthermore, Fig. A1 suggests that there is a great degree of overlap between the two night definitions, as far as the mean CO_2 flux is concerned. As one can see, on average, the CO_2 flux transits zero somewhere near $+5$ degrees threshold that we have defined. At the same time, when the PAR threshold of $10 \text{ } \mu\text{mol m}^{-2} \text{ s}^{-1}$ is used, an equivalent number of negative CO_2 data are marked as “night”. So, we suggest that the two methods of night period definition produce approximately equivalent results. Nevertheless, we are using the PAR definition in the revised manuscript.

420

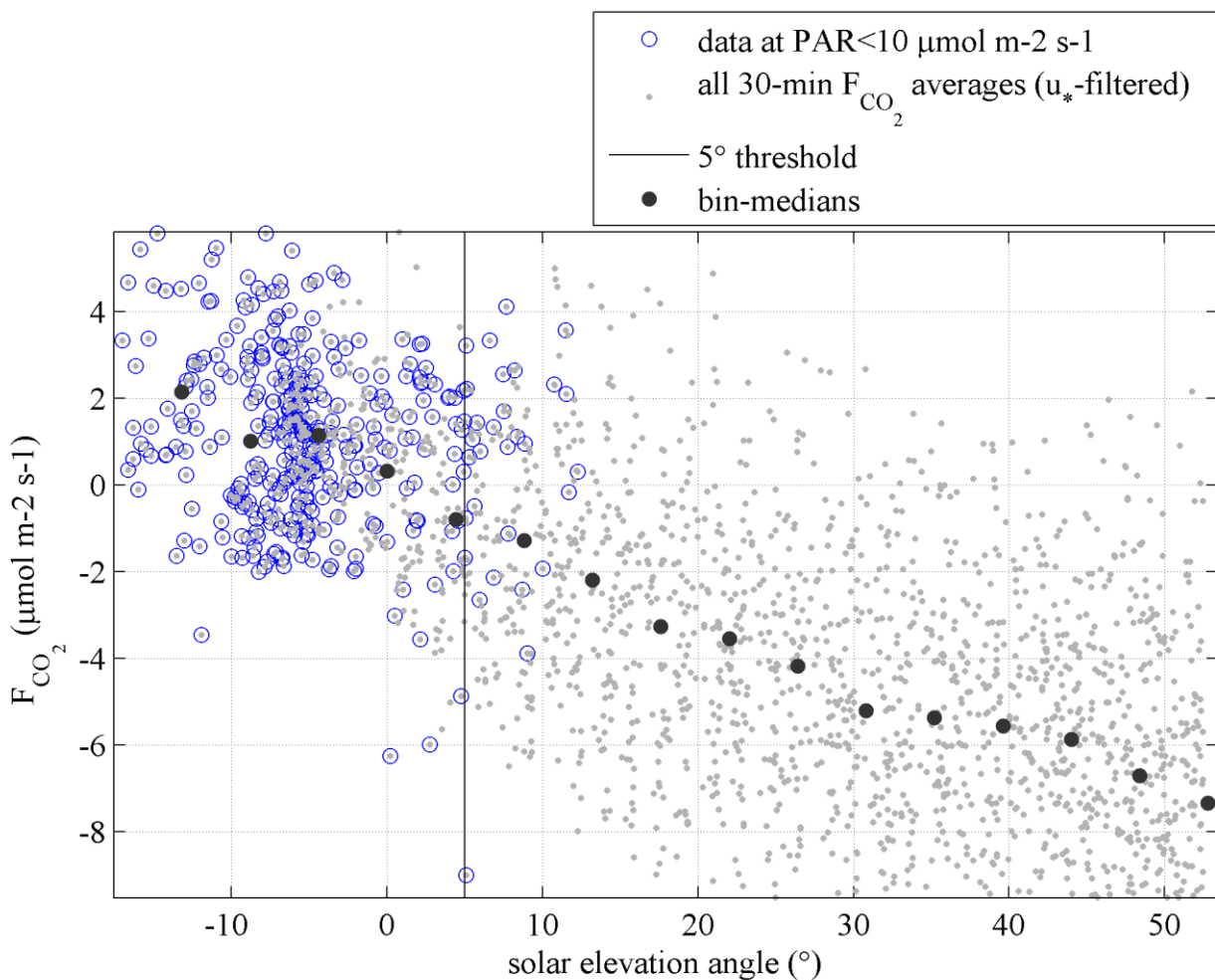


Fig.A1. EC CO_2 flux versus solar elevation angle.

425

L 206 Did you try to use other soil temperatures than at 5 cm depth to model the respiration? Please include R2 to the Figure 3.

Yes, we did. It was difficult to find any improvement when the other temperature measurements were tried. In the revision, we are using the area-weighted average of the ridge and hollow -5cm temperatures, so that to account for the spatial variation.

430

The original Figure 3 proved to be confusing and gave a wrong idea that the displayed “general” fits were used to model Re and GPP for the whole period, therefore, it was replaced with the parameter timeseries figure. We did not use the general regression of peat temperature to Re anymore, as described in the description of the revised gapfilling method.

435 In any case, the requested R2 of the Tp-Re fit in former Figure 3a was 0.55.

L234-236 You use just the soil temperature at 5 cm depth for modelling, please include this information to the text and skip the information on soil temperatures at other depths.

440 We would maybe argue that the 20 and 50 cm depths be kept, once again for the reason that it has not been published anywhere, while it might interest some as background. The 20 and 50cm depths are added to Fig. 4a in the revision.

L 310-311 So the range of the values in the Fig 8a show just values from +3 to -9 mol/m2s.

445 This is correct. We did zoom into the main data cluster so that to make the seasonal dynamics clearer. The extreme 30min averages in fact do not need to be mentioned, as they represent the typical random variability of the eddy-covariance fluxes rather than the typical exchange, which is bounded by about +5 and -10 umol/m2s.

L 312 The vegetation might play an important role as well.

450 You are absolutely right, we should mention this biological driver along with the abiotic ones, temperature and PAR. However, the LAI or other vegetation parameters have not been directly measured at the site.

L 318 Please include the gapfilling methods for the NEE fluxes.

455 We agree on the importance of this information; we hope that the revised section 2.6 provides sufficient detail on the gapfilling method.

L 329 What was the range of daily fluxes in Mukhrino?

460 For June-August, the average daily cumulative NEE was -1.8 g C m-2, so, well within the values observed elsewhere. This estimate is included in the revised text for a clearer comparison with the literature.

L 351 It might be interesting to include a figure with a typical diurnal course before and during the passage of the weather front.

465 It should be possible to add show a close-up of the daily course as an extra panel to Fig.8. This addition is made in the revised MS. The third front passage period having the least proportion of gaps is displayed as a case study.

470

475

480

Response to Review #3

485

Anonymous Referee #3

Received and published: 5 April 2017

490

The paper by Alekseychik et al. presents the first data collected by an eddy covariance tower near the Mukhrino field station in West-Siberia. Since there are very few eddy covariance towers in this part of the world, I'm confident that the data collected will be of great interest to a wide audience, including modelers that wish to test their simulations. However, the station has not yet been operational for a long time and this study therefore only presents the first four months of data.

495

Unfortunately, this also means that little new scientific knowledge on the processes governing carbon exchange is presented in this paper apart from adding an extra data point on the map (although data from understudied areas is valuable in itself, obviously).

We thank you for your appreciation of our work and acknowledging the novelty of the study. We certainly are planning to continue the measurements in as continuous a manner as it will be possible.

500

As the first paper from a new field station, it is important that the description of the data collection is complete and accurate, since it will be the reference paper for future studies from this location. But in order to achieve that, several improvements need to be implemented. Many of such remarks were already made by the other two referees, and I will therefore not delve too long on the areas where our reviews overlap. First of all, it is not clear why the gapfilling and partitioning of the data has not been done by more common methods provided by the Fluxnet community. I suggest to do the partitioning and gapfilling of NEE according to Reichstein et al. (2005). The scripts to do so are freely available on the Fluxnet website. Following common Fluxnet methodology is important to include this new station as a valuable point of reference, and it would be helpful to point out where calculations are similar to previous studies, and where they diverge. Reference to Aubinet et al. (2001) or the later book from Aubinet et al. (2012) are useful in that regard.

505

510

515

We understand the concern. The modeling/partitioning method has been updated in the revised manuscript, and the explanation can be found in the response to a comment by Reviewer 1. The new method improves the models by accounting for the seasonal change in the respiration parameter R_{ref} .

However, given such a challenging dataset, the strict application of the Fluxnet methods seems problematic, as those methods function more optimally with more complete datasets. This was acknowledged by Reichstein et al. 2005:

520 “To sum up, the algorithm introduced here was able to find a short-term temperature response of
Reco at all studied sites and is a significant step forward towards less biased estimates of Reco and
GEP. Nevertheless, important limitations should be noted: It is not guaranteed to work at all sites
since whether one can find a reliable short-term relationship between Reco and temperature
depends on the noisiness of the eddy data and the range of temperatures encompassed during the
525 short period. At sites with very stable temperatures and noisy eddy covariance data, it might be
possible that within a year no short period can be found where a temperature–Reco relationship can
be established at all. Seasonal changes in the temperature sensitivity that have been hypothesized
are hard to detect from eddy covariance data, since in many cases not enough shortterm periods
with a good correlation between temperature and Reco were found to make up a seasonality.”
530 We have to admit that our data is noisy in exactly this sense, and, in addition, it is full of gaps,
especially during the nights.

Nevertheless, we believe that our approach to Re and GPP modeling works towards the same ends
as that of Fluxnet, while being at the same time optimized for our dataset.

535 Also, as pointed out by the other referees, the paper does not present vegetation data and assumes
too much about the phenology of the vegetation. If this data is unavailable, that would be a pity,
since it would help a lot more to explain the data. Care needs to be taken to acknowledge that data
gap, if it exists, and to not over-interpret the data.
540 Unfortunately, LAI has not yet been determined at the site.

Figure 1d shows that the area within the footprint has quite a bit of variance. The heat fluxes are
integrated over this footprint, while soil temperature and net radiation measurements are taken in
one point. An energy balance closure of 90% is then very high, given the fact that the different
545 energy fluxes are not measured on the same area. The one place where some wiggle room remains
is in calculation of the heat flux, which is highly dependent on the volumetric heat capacity of the
soil in equation 4. Yet, soil properties are not mentioned in the paper and simply assumed to be 95%
water and 5% peat, according to a reference from 1999. How realistic is this assumption and would
your energy balance be worse if it was 80% water and 20% peat, to name just a number? Some
550 uncertainty assessment of the assumptions behind the calculated soil heat flux would be preferable
and show how this relates to the energy balance closure.

The 95% porosity in the top 50 cm of peat was originally adopted from Yurova et al. 2007, whose
model was used to predict the profile of volumetric water content based on water level, as we
lacked direct observations of water level. The Yurova et al. model was parameterized for the
555 porosity values ranging from 92 to 98% between catotelm and acrotelm, so we assumed that 95%
would represent the mean conditions well enough. However, at the time we were preparing this
manuscript, the new results on the physical properties of peat at Mukhrino were not yet available.
Szajdak et al. (2016) summarized their measurements in six representative micro-landscapes around
the site and found an average porosity in the top 50 cm of peat to be 93%. Therefore, our earlier
560 assumption of 95% porosity in surface peat layer was realistic. To be consistent with Szajdak et al.
(2016), we will update the porosity value.

The other reviewers suggested to recalculate soil heat flux as an area-weighted average of the fluxes
calculated for hummocks and hollows, which we do in the revised MS version. As Szajdak et al.
(2016) do not present microform-specific results, we will be forced to use the same 93% porosity
565 for both microform types.

Page 2, line 61: It would be good to include a more precise location of the tower, rather than these
rounded coordinates, for future reference and model work.

Will be done. The precise coordinates of the EC tower are given on the line 126 in the revised MS.

570

Page 4, line 115: please mention the exact dates here also, and not only later in the document.
Done.

575

Page 6, line 169: is G calculated from the soil temperature measurements at 2, 5, 10, 20 and 50 cm depth? Please specify.

It was calculated from the temperature measurements at 5, 10, 20 and 50 cm depths. This will be specified. The 2 cm level was omitted because there was no certainty that it shows the peat (moss) but not air temperature, i.e. that the sensor was constantly in a good contact with the vegetative parts or soil.

580

Page 6, line 179: how well would this equation work for this site? Seems to me that volumetric water content would vary a lot between ridges and hollows.

The Yurova et al. 2007 model was constructed for a Swedish fen, which closely resembles the lawn microsities of Mukhrino. Lawns-hollows being the dominating microform in the areal sense, the equation probably describes the average water content over most of the area with satisfactory precision. In the revision, the hollow and ridge WTD data are used separately to model water content profile for these microsite types.

585

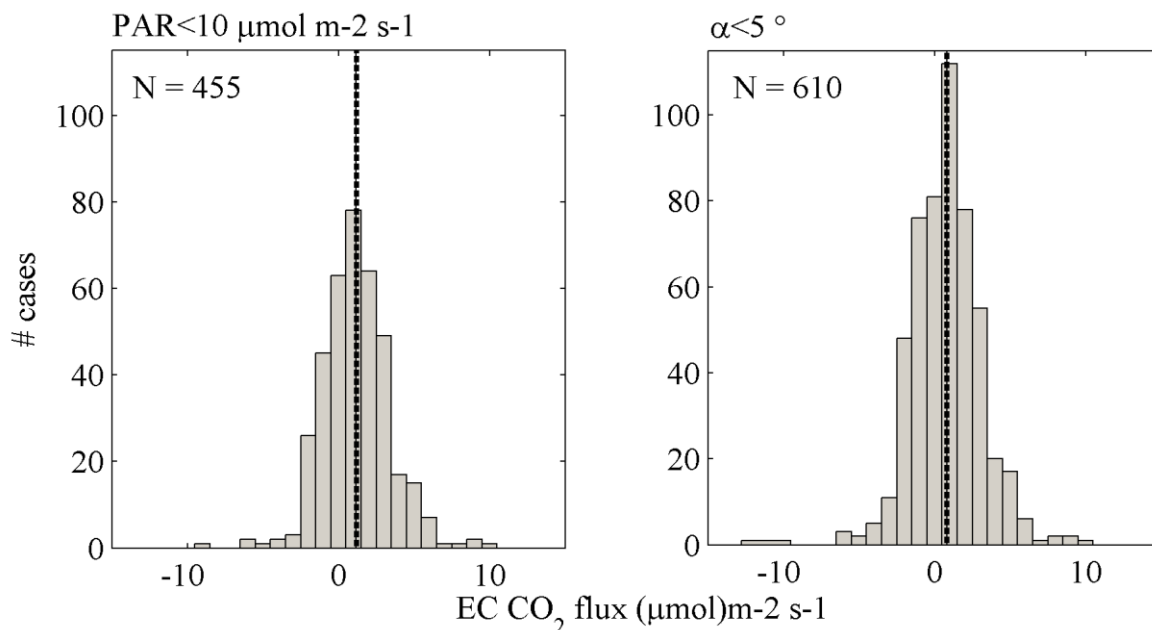
590

Page 7, line 206: as mentioned by the others, why not simply look at measured PAR as a threshold? Was the sensor shaded by trees?

The CO₂ flux distributions at the two night definitions are more or less identical (Fig. R1). These data are u*-filtered. As with the of the open-path sensors in general, our nighttime flux is characterized with high random uncertainty. Both definitions yield realistic mean nocturnal CO₂ flux of about +1 $\mu\text{mol m}^{-2} \text{s}^{-1}$, have similar shapes and kurtoses. However, the definition based on solar angle leads to more nocturnal periods than the PAR definition (610 versus 455).

595

In any case, we are using the PAR definition of nighttime periods in the revision, as the new CO₂ flux model is not as sensitive to the amount of nighttime data, as its previous version.



600

Fig. R1. Histograms of eddy-covariance CO₂ flux for the two alternative night definitions, based on PAR (left panel) and solar angle (right panel).

Page 7, line 210: fitting this equation on all data at once leads to a very uncertain fit, as is clear from Figure 3a, due to temporal variation in the base parameters. The method by Reichstein et al. (2005) therefore shifts short optimization windows throughout the season. Something similar should've been applied here, since Q10 is probably not stable and depends on changes in e.g. soil moisture and substrate availability.

As discussed in the response to the previous comment, the number of nocturnal data is very low, and this prompted us to use that simplified approach. Representation of the seasonal course in Q10 seems challenging for this dataset, however. However, we found a way to circumvent the problem by representing the seasonality in the Rref parameter. This is done in a way similar to the Reichstein et al. 2005, although not down to fine detail. The limitation of the data coverage has played a major role in the choice of the gapfilling method, however we hope that we reach similar targets as Reichstein et al. 2005.

Page 7, line 216: same as previous remark. Why fit this to the entire dataset when the phenology of the plants, and therefore base parameters, is changing throughout the summer? There are better partitioning methods out there.

We must have described the gapfilling scheme in a confusing way, apologies for this. In fact, the other reviewers were similarly puzzled about this point. Fig. 3 shows a fit to all data together just for demonstration. What actually was done, is the estimation of the GPP model parameters (Pmax and k) in a 1 month-wide moving time window moved in 1-day steps. Smoothed timeseries of Pmax and k were then obtained from these daily estimates. So, our approach does capture the vegetation phenology and other seasonal effects. Please see Fig. R1, which was also included in our response to Review 1. The updated CO2 flux gapfilling method is described in the revised MS section 2.6.

Page 8, line 231: 'dramatic' is a subjective term. Perhaps this is normal in this area?

We wished to underline the dramatic nature of snowmelt in the year 2015, as it really was beyond the normal – early and rapid. In the revised manuscript, we rephrase it as “an unusually early and rapid snowmelt in April and the beginning of May”.

Page 10, line 259: 'probably'? how would you know if you haven't measured this? Isn't the lower amount of incoming PAR the reason that Rn is also lower?

At the time of this response' writing, we can confirm this suggestion with data. We do observe a summer minimum in PAR albedo in early July (about 4%). After that, PAR albedo climbs to 6-7% by mid-August. However, while the short-term variations in PAR albedo are correlated with the heavy rain periods, the absence of strong seasonal trend in WTD does not allow to view it as a driver of PAR albedo in that year. Instead, the late summer increase in albedo must have been due to the senescence of vascular vegetation. Although albedo for global radiation was not measured, one could surmise that it followed similar trends.

Finally, Rn reduction solely due to change in albedo was meant here (line 259). Of course, this occurs in parallel with the downward trend in insolation after the summer solstice.

Page 10, line 260: incoming solar radiation is logically lower in August, since it's further removed from midsummer. So this would also happen if there was no difference in cloud cover.

We fully agree. As in the previous point, the individual effect of cloudiness was meant, as an addition to the astronomical component in solar radiation variation. We are sorry that this was not stated clearly, and it will be rephrased.

Page 14, line 345-347: This sentence is unclear. Are you talking about this in general terms or are you referring to this site?

655 If we understand this comment correctly, yes, we are discussing the effects of the fronts in terms of the *in situ* observations. The water table dynamics discussion in Price (2003) is of general relevance, and only used as a theoretical framework for the particular case of Mukhrino.

Page 15, line 364: The landscape in your footprint doesn't look homogenous at all, with all the variation between ridges and hollows. It's just that this variation is similar within different areas of your footprint, but that's not the same as homogeneity.

660 We agree with this note. This landscape is homogeneous on the length scales of 100 m and more, but it could be incorrect to call it homogeneous in a common sense (as in the Degerö which is devoid of any small or large scale features, e.g. Peichl et al. 2013).

Figure 10: how was does normalizing done? Please explain.

665 The observed flux was simply divided by the model. We will make this more specific in the text.

Page 16, line 384: Are these observations really in these IPCC reports? Surely, there's a peat synthesis product out there that can be cited instead.

670 It actually the "Supplement to the 2006 IPCC Guidelines for National Greenhouse Gas Inventories: Wetlands" we are referring to. IPCC themselves suggest referring to it as "IPCC 2013, 2014".

Quoting the IPCC website (<http://www.ipcc-nggip.iges.or.jp/public/wetlands/>):

675 "Please cite as: IPCC 2014, 2013 Supplement to the 2006 IPCC Guidelines for National Greenhouse Gas Inventories: Wetlands, Hiraishi, T., Krug, T., Tanabe, K., Srivastava, N., Baasansuren, J., Fukuda, M. and Troxler, T.G. (eds). Published: IPCC, Switzerland"

Page 16, line 388: You cannot say 'apparently' since you are not reporting the course of vascular plant leaf area development.

680 LAI was not measured and we can only surmise about its effects. However, the Pmax course (Fig. R2) should approximately correspond to the LAI seasonal curve. But we agree that using "possibly" or "likely" would suit this sentence more than "apparently".

685 References

Granberg, G., Grip, H., Löfvenius, M. O., Sundh, I., Svensson, B. H., and Nilsson, M.: A simple model for simulation of water content, soil frost, and soil temperatures in boreal mixed mires, *Water Resour. Res.*, 35, 3771-3782, 10.1029/1999WR900216, 1999.

690 Peichl, M., Sagerfors, J., Lindroth, A., Buffam, I., Grelle, A., Klemedtsson, L., Laudon, H. and Nilsson, M.: Energy exchange and water budget partitioning in a boreal minerogenic mire, *J. Geo.Res.*, 118, 1-13, 2013.

Szajdak L.W. et al. 2016. Physical, chemical and biochemical properties of Western Siberia. *Environmental dynamics and global climate change*. 2016. 7, pp. 13–25.

695 Yurova, A., Wolf, A., Sagerfors, J., and Nilsson, M.: Variations in net ecosystem exchange of carbon dioxide in a boreal mire: Modeling mechanisms linked to water table position, *J. Geophys. Res.: Biogeosciences*, 112, 10.1029/2006JG000342, 2007.

700

Net ecosystem exchange and energy fluxes ~~in a West Siberian bog~~ measured with eddy covariance technique in a West Siberian bog

Pavel Alekseychik¹, Ivan Mammarella¹, Dmitri Karpov², Sigrid Dengel⁶, Irina Terentieva³, Alexander Sabrekov^{2,3}, Mikhail Glagolev^{2,3,4,5} and Elena Lapshina²

¹Department of Physics, P.O. Box 68, FI-00014, University of Helsinki, Finland

²Department of Environmental dynamics and global climate change, 628012, Yugra State University, Russia

³Tomsk State University, Russia

⁴Department of Soil Physics and Development, 119991, Moscow State University, Russia

⁵Institute of Forest Science, Russian Academy of Sciences, 143030, Moscow, Russia

⁶Climate and Ecosystem Sciences Division, Lawrence Berkeley National Laboratory, Berkeley, USA

Correspondence to: Pavel Alekseychik (pavel.alekseychik@helsinki.fi)

Abstract. Very few studies of ecosystem-atmosphere exchange involving eddy-covariance data have been conducted in Siberia, with none in West Siberian middle taiga. This work provides the first estimates of carbon dioxide (CO₂) and energy budgets at a typical bog of the West Siberian middle taiga based on May-August measurements in 2015. The footprint of measured fluxes consisted of homogeneous mixture of tree-covered ridges and hollows with the vegetation represented by typical sedges and shrubs. Generally, the surface exchange rates resembled those of pine-covered bogs elsewhere. The surface energy balance closure ~~was approached 100%~~ 90%. Net CO₂ uptake was comparatively high, summing up to 202 gC m⁻² for the four measurement months, while the Bowen ratio was ~~typical at~~ seasonally stable at 283%. The ecosystem turned into a net CO₂ source during several front passage events in June and July. Several periods of heavy rain helped keep the water table at a ~~constant~~ sustainably high level, preventing a usual drawdown in summer. However, because of the cloudy and rainy weather, the observed fluxes might rather represent the special weather conditions of 2015 than their typical ~~level~~ magnitudes.

1. Introduction

Boreal peatlands, covering a large fraction of the northern hemisphere, are an important terrestrial carbon pool, whose size is estimated to be around 500 ± 100 Pg of organic carbon when integrated over the entire peat depth (Yu, 2012).

740 Photosynthesis and respiration of plant and microbial communities regulate the size of this pool. However, peatlands are also prone to rapid ecological changes related to climate, which modify the interaction between hydrology, carbon cycle, vegetation cover and micro-topography. Detailed knowledge of the processes governing the carbon exchange in northern peatlands over the course of a growing season is limited, especially with respect to the impact of relevant environmental variables.

745 While continuous and long-term time series of carbon dioxide (CO₂), sensible and latent heat fluxes are already available from several boreal peatland sites in Europe, measurements of this kind are rare in Siberia. The closest permanent West-Siberian bog installation is part of the ZOTTO facility (Heimann et al. 2014), while other comparable stations are found in European Russia (Ust Pojeg - Gazovic et al. 2010), Finland (Tervalamminsuo – Annalea Lohila, personal communication; Siikaneva bog site - Korrensalo et al. 2017), Sweden (Fäjemyr - Lund et al. 2007), and Canada (Mer Bleue - Humphreys et al. 2014). This is mainly due to the lack of developed measurement sites with the
750 infrastructure suitable for continuous monitoring of the ecosystem-atmosphere exchange processes, and frequent general inaccessibility of key ecological zones and biomes. In remote and large areas such as West Siberia, current estimates of greenhouse gas emission-exchange rates are largely uncertain, because discontinuous and short-term observations (static chamber technique) have often been used to derive regional and long term emission-exchange rates (Golovatskaya and Dyukarev, 2008;Schneider et al., 2011;Glagolev et al., 2011;Sabrekov et al., 2013). Currently, only
755 about ten eddy-covariance (EC) flux tower sites are active in Russia east of the Urals (Alekseychik et al., 2016). No prior publications of eddy-covariance fluxes from the West-Siberian peatlands are known to the authors. Previous studies using-utilising this-the EC method in Boreal peatlands elsewhere have shown the importance of temperature, solar radiation, and water table depth in controlling the net ecosystem exchange (NEE) (Arneth et al., 2002;Aurela, 2004;Lafleur et al., 2003;Friborg et al., 2003;Humphreys et al., 2006). Most studies show that, during the growing
760 season, peatlands are-typically act as net sinks for-of CO₂. However, during warm and dry growing seasons the peatland sink strength is notably reduced and in some cases lead to net CO₂ losses (Bubier et al., 2003;Lafleur et al., 2003).

In order to fill the West Siberian measurement gap, we have recently established a new EC flux tower at the raised bog site at the Mukhrino field station in Khanty–Mansi Autonomous Okrug (Russia). The Mukhrino field station is officially part of the PEEEX station network (Alekseychik et al., 2016) and INTERACT (<http://www.eu-interact.org/>).
765 The energy and carbon dioxide flux data provided by the eddy-covariance tower is so far unique for West Siberian middle taiga and is the only setup functioning as of 2016 in West Siberia (within at least a radius of 1000 km). The aims of this study are to present and analyze the new flux data tower with the related ancillary measurements, to investigate the diurnal and seasonal variations of NEE and energy fluxes, as well as to determine summertime budgets of energy and CO₂ of the ecosystem.

770 **2. Materials and methods**

2.1 Site description

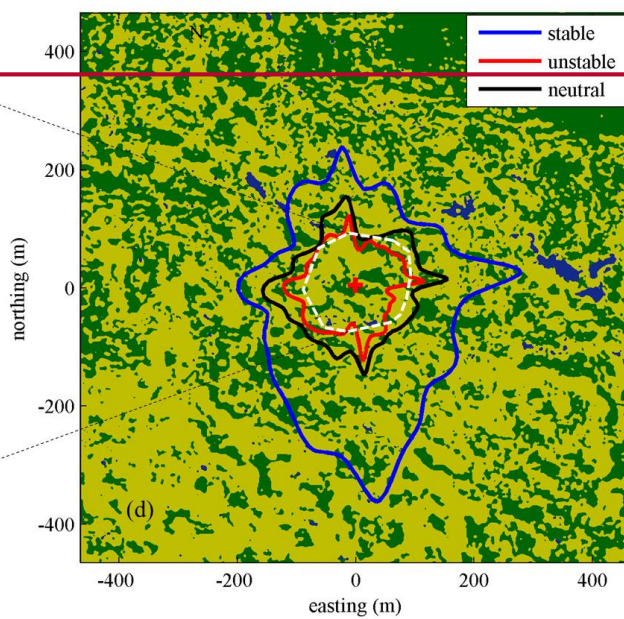
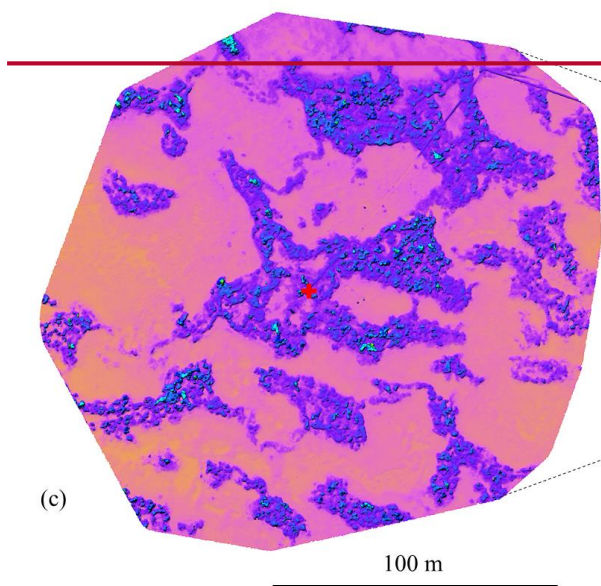
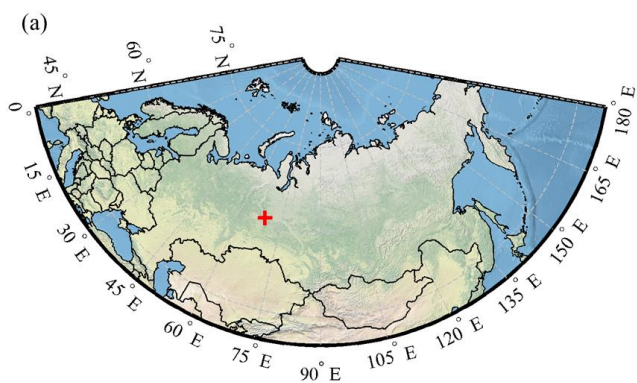
The Mukhrino Field Station (60°54' N, 68°42' E) is located at the eastern terrace of the Irtysh River 20 km south of the point of confluence with the Ob' river, in the middle taiga zone of the West Siberian Lowland (WSL). West Siberian
775 Lowland WSL is a geographical region of Russia bordered by the Ural Mountains in the west and the Yenisey River in the east; the region covers 2.75×10⁶ km² from 62-89° E to 53-73° N. Paludification in West Siberian Lowland WSL started after a climate warming 11500 cal. BP, with 55% of the present C store accumulated by 6 000 cal. BPP; The mires have expanded very little during the past 3000 years (Turunen et al., 2001). The mMiddle taiga ecozone (59-62°

780 N) covers an area of about $0.57 \times 10^6 \text{ km}^2$ ~~56.6 Mha~~ in the central part of the West Siberian Lowland~~WSL~~; the region features flat terrain with elevations of 80 to 100 m above sea level.

785 The region has a subarctic or boreal climate (Köppen-Geiger code Dfc) with ~~a~~-long cold winter, ~~a~~ short warm summer and frequent change of weather conditions. Average monthly air temperatures range from -20 to 18 °C over the year with the mean annual temperature of -1.1 °C. The latter increased by 0.4 °C from 1893-1935 to 1970-1999 period (Bulatov, 2007). Median annual precipitation is 520 mm, and evapotranspiration is 445 mm (Bulatov, 2007). Mean summer precipitation is 208 mm, ranging from 74 mm to 354 mm over the period from 1934 to 2014. ~~Continuous~~ Permafrost in any form is absent. Peat soils freeze to a depth of about 50 cm. Typically, snowmelt and river break up start in the first half of May. Mean duration of snow cover period is 180 days (from 19 October to 25 April) with the average March snow depth 54 cm. Growing season lasts for 98 days (Bulatov, 2007); the number of growing degree-days >5 °C is from 900 to 1500 (median – 1250).

790 The excess water supply and flat terrain with poor drainage provides favorable conditions for wetland formation in the region. Large wetland systems commonly cover watersheds (34% of the zonal area) and have a convex dome with centers that are 3 to 6 m higher than the periphery. The wetland subtypes here have strict spatial regularities. Ridge-hollow-lake complexes (15% of the total wetland area) represent central plateau depressions with stagnant water. They consist of numerous small lakes up to 2 m deep with peat bottom and waterlogged hollows. Different types of ridge-hollow complexes dominate (42%), covering the better drained gentle slopes. Pine bogs (28%) are more frequent in drier areas, where the peat surface is typically 10-50 cm above the water table level. Poor and rich fens (8%) develop along the wetland edges and watercourses, where the nutrient availability is higher. Open bogs with mosaic dwarf shrubs-sphagnum vegetation are widespread (5%) at the periphery of individual wetland bodies. Wooded swamps (2%) surround the peatland systems (Terentieva et al., 2015). Primary lakes of 100-2000 m in diameter and up to 5 meters

800 depth with mineral bottom are widespread.



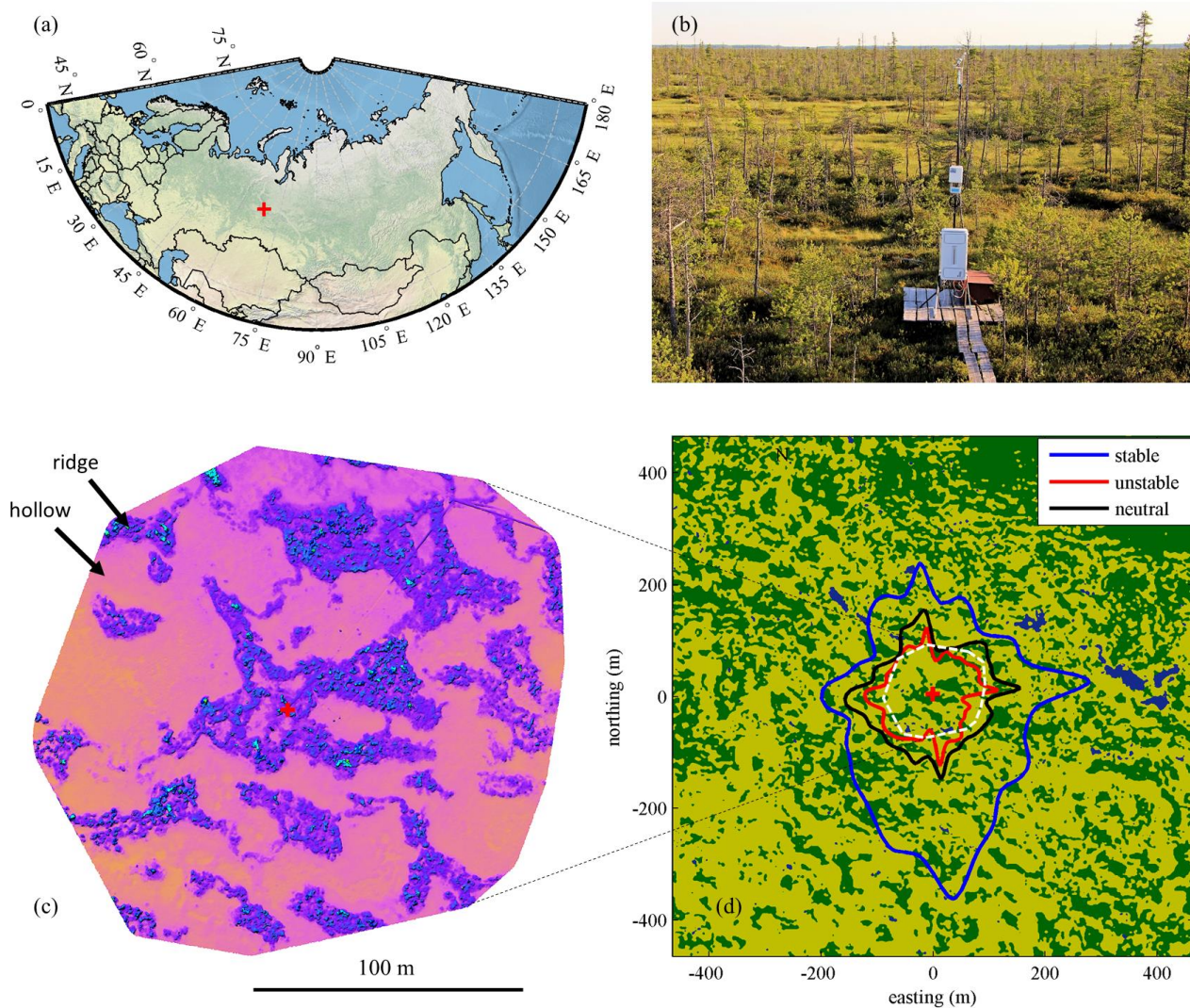


Figure 1: (a) map showing the Mukhrino station location, (b) photo of the EC tower facing southwest, (c) digital elevation map based on drone survey, (d) surface type classification map. (d) includes an eddy-covariance footprint overlay, with the isolines ~~delineating~~ ~~giving~~ the 70% cumulative EC source zone in the three stability classes. Color coding in (d): dark green – ridges/hummocks, light green – lawns/hollows, dark blue – ponds. The red cross marks the location of the EC tower.

The Mukhrino Field Station (map, Fig. 1a) is located on the eastern edge of a peatland 10 km × 5 km size. The study site is considered to be representative of raised bogs, a peatland type dominant not only in the west (Masing et al., 2010), but also in the other parts of Siberia (Shulze et al., 2015). ~~It has a~~ ~~The~~ peat layer of up to 5 meters in depth ~~that~~ is composed of Sphagnum ~~peat~~ with minor contributions by other plants. ~~The Mean~~ pH is ~~from 3.5~~ ~~to~~ 5, electric conductivity – from 0 to 200 $\mu\text{Sm}/\text{m}^2$ (Sabrekov et al., 2011). The rate of peat accumulation at ~~the a~~ nearby ~~wetland~~ ~~wetland site~~ was 0.35 mm yr^{-1} , while the average dry bulk density of the peat was 92.7 g dm^{-3} with the average C peat content of 52.7% (Turunen et al., 2001).

Pine bogs and ridge-hollow complexes are dominant within the boundaries of Mukhrino bog (Fig. 1b-d). The tree cover of ridges and pine bogs is represented by stunted *Pinus sylvestris*. The ~~i~~ dwarf shrub layer consists of *Ledum palustre*, *Andromeda polifolia*, *Chamaedaphne calyculata*, *Vaccinium vitis-idaea*, *Vaccinium uliginosum*, *Oxycoccus palustris*.

820 Herbs are represented by *Rubus chamaemorus* and a few tiny species of sundews (*Drosera anglica*, *D. intermedia*, *D. rotundifolia*). *Carex limosa*, *Eriophorum vaginatum*, *Scheuchzeria palustris* are widespread within oligotrophic hollows of ridge-hollow complexes. The moss layer of raised bogs consists of Sphagnum mosses as *S. fuscum*, *S. lindbergii*, *S. balticum*, *S. papillosum*, *S. angustifolium*, *S. magellanicum*, *S. jensenii*, etc. The area fractions of open water, hollows and ridges within a 200_m radius around the flux tower are 1%, 67% and 32%, correspondingly (Fig. 1c-d).

825 Over the past years, the Mukhrino bog has been ~~the-in the~~ focus of a large number of studies ranging from surface-atmosphere gas exchange (Glagolev et al., 2011) to geochemistry and physical, chemical and biochemical properties of peat (Stepanova and Pokrovsky, 2011; Szajdak et al., 2016), hydrology (Bleuten and Filippov, 2008), microbiology including mycology (Filippova et al., 2015).

2.2 Measurements

830 Turbulent fluxes of momentum, sensible (H) and latent (LE) heat, and CO₂ were measured between 1st May and 2nd September 2015 with the eddy-covariance (EC) technique. The EC system included a 3-D ultrasonic anemometer (Gill R3, Gill Instruments Limited, Great Britain) providing three wind velocity components and the sonic temperature, and an open-path infrared gas analyzer (LI-7500, LI-COR Biosciences, USA) for the measurement of CO₂ and water vapor (H₂O). The EC sensors were mounted on a tower at a 4 m height above the peat surface. The horizontal separation
835 between the sonic anemometer and the gas analyzer was 15 cm. The open-path gas analyzer was connected to the analogue input of the sonic anemometer. ~~The d~~Data were logged on a mini-computer via ~~serial cable~~ using a mini-computer ~~at with the~~ sampling frequency of 10 Hz. The eddy-covariance tower coordinates are 60.89133° N, 68.67627° E.

840 Auxiliary parameters were measured and recorded by two automatic meteorological stations located within 30 m from the EC tower. The measured parameters include the soil temperature profiles s at depths of 2, 5, 10, 20 and 50 cm (thermocouple sensors), net radiation (Kipp&Zonen NRLite radiometer), incoming and reflected photosynthetically active radiation (Li-Cor LI-190SA Quantum Sensor), air temperature and relative humidity (ROTRONIC HygroClip S3) and precipitation (HOBO Data Logging Rain Gauge RG3-M). The soil temperature profiles were installed in ridge and hollow, two replicates in each microsites; the replicates were averaged for further uses. Water table level was also
845 measured in both types of ~~microsites measured in two locations (hollow and ridge) by with~~ two Mini-Diver ~~water level~~ sensors (DI 501).

The station uses an autonomous power supply system consisting of solar panels (4 kW in total) and a wind vane generator (3 kW). A combined charge controller/invertor unit charges the batteries with the total capacity of 800 Ah and supplies up to 3 kW to the field station. In wintertime, a 2.5 kW petrol generator is additionally used.

850

3. Methods

23.31 Flux calculation

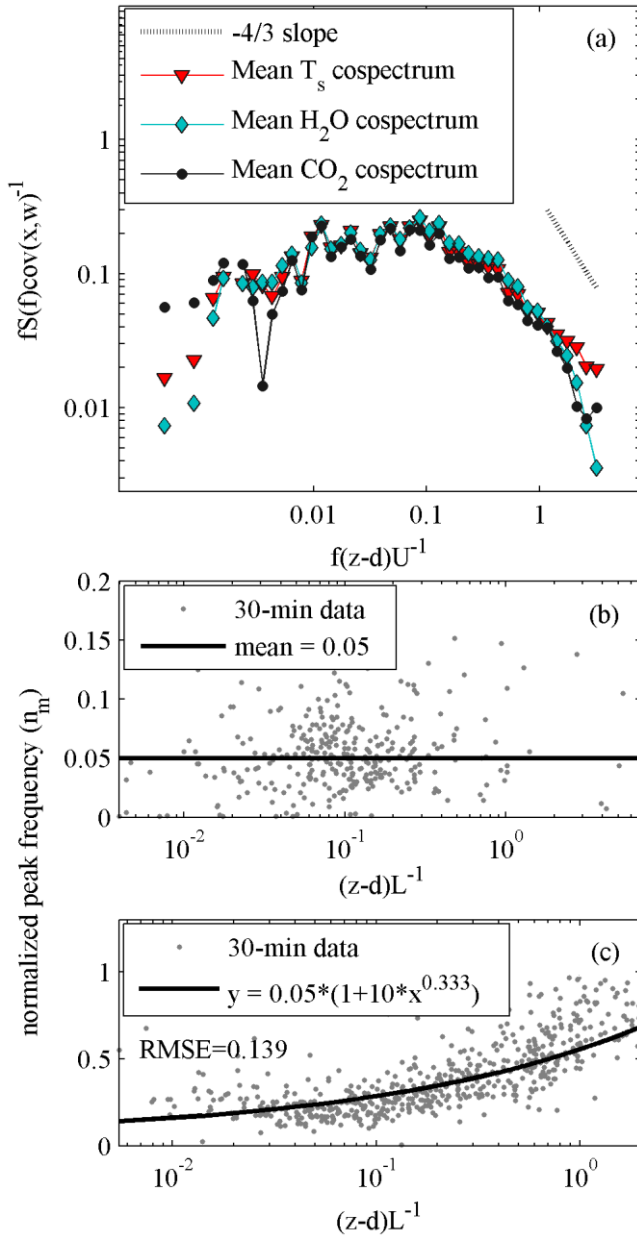


Figure 2: (a) Normalized frequency-weighted co-spectra of temperature, carbon dioxide and water vapour as a function of normalized frequency measured on 16 July 2015, 11:00-13:30 (mean value of stability parameter $(z-d)L^{-1} = -0.023$). The two following subplots show the 30 min values of the normalized peak frequency n_m versus the stability parameter $(z-d)/L$ in unstable condition (b) and stable conditions (c).

The post-field processing of EC rawdata was performed with EddyUH software (Mammarella et al., 2016). Fluxes of sensible and latent heat and CO_2 were calculated as the 30-min block-averaged covariances between the scalars and the vertical wind velocity:

$$H = \rho_d c_p \overline{w' T_a'} \quad (1)$$

$$LE = \rho_d L_v \frac{M_w}{M_a} \overline{w' \chi_{H_2O}'} \quad (2)$$

$$F_{co_2} = \frac{\rho_d}{M_a} \overline{w' \chi_{CO_2}}, \quad (3)$$

865

where ρ_d is the dry air density (kg m^{-3}), c_p the specific heat capacity of dry air ($\text{J kg}^{-1} \text{K}^{-1}$), L_v is the latent heat of vaporization for water (J kg^{-1}), T_a the air temperature (K) and M_a and M_w the molar masses of dry air and water, respectively. The terms $\overline{w' T_a'}$, $\overline{w' \chi_{H_2O}'}$ and $\overline{w' \chi_{CO_2}'}$ are the covariances between w and T_a , dry mole fractions of CO_2 and H_2O , respectively.

870

Data were de-spiked according to standard methods (Vickers and Mahrt, 1997), thereafter wind velocity components were rotated into a natural coordinate system by performing a two-step rotation to each 30 min interval setting the x axis along the mean wind direction and zeroing the mean vertical wind velocity. The time delay between the vertical wind speed w and the scalar (CO_2 or H_2O) was derived for each 30 min interval by maximizing the respective cross-correlation function, calculated in a very narrow window (from -0.5 s to 0.5 s). The fluxes were corrected for high and low frequency losses that occur due to the limited frequency response of the EC system and the finite time averaging period used for calculating the fluxes, respectively. Correction was done according to Mammarella et al. (2009) by using experimentally and theoretically determined co-spectral transfer functions at high and low frequency. The estimated low pass filter time constant for CO_2 and H_2O was 0.05 s. The effect of this correction is very small, and is mainly caused by the separation between the open-path analyzer and the sonic anemometer. The high frequency attenuation can be clearly seen in the measured co-spectra (Fig. 2a). When performing the spectral correction to the CO_2 and H_2O fluxes, the derived transfer functions were used together with the site-specific co-spectral model, which was estimated by a non-linear fit of the measured $\overline{w' T'}$ co-spectrum. The normalized frequency of the co-spectral peak (n_m) was also estimated from the co-spectrum for each 30 min record, and the site-specific stability dependence was established (Fig. 2b-c). In unstable conditions (stability parameter $z/L < 0$) n_m has a constant value of 0.05, whereas in stable conditions an increase with atmospheric stability is observed ($z/L > 0$). Before calculating the sensible heat flux, the 30 min sonic temperature covariances are converted to actual air temperature covariances following the approach of van Dijk et al. (2004). ~~Finally,~~ LE and CO_2 fluxes are corrected for air density fluctuations (Webb et al., 1980). ~~Finally,~~ the Burba correctinon (Method 4 in Burba et al., 2008) was applied to the CO_2 and LE fluxes.

890

Ground heat flux (G) was calculated ~~from for the ridge and hollow microforms from~~ the peat temperature profile as heat storage change in the top 50 cm of soil following the methodology described in Ochsener et al. (2007) and elsewhere:

$$G = \int_0^{50\text{cm}} C_v \frac{\partial T}{\partial t} dz \quad (4)$$

895

The total volumetric heat capacity, C_v , was calculated as a sum of volumetric heat capacities of the solid, water and air constituents, weighted by their volume fractions in the soil matrix. The temperature measurements at 5, 10, 20 and 50 cm depths were used here. Volumetric soil water content profile was modeled as a function of water level (Yurova et al., 2007; Weiss et al., 1998):

900

$$\theta(z) = \phi[1 + (a(-(WT - z)))^b]^{-1+1/b} \quad (5)$$

where ϕ is the soil porosity and a, b the empirical parameters. ϕ was taken as 95%, corresponding to the average of the representative acrotelm and catotelm values (Granberg et al., 1999). Therefore, the fraction of solid peat particles constituted the remaining 5% of the volume. a and b were adopted from Yurova et al. (2007). The ridge and hollow WT measurements were used to model θ for two microsite types. Finally, a footprint-representative estimate of G was obtained as an average of the ridge and hollow fluxes weighted by the respective area fractions (68% and 32%).

23.42 Flux quality criteria and footprint

In this study, we analyzed the ~~EC~~-data ~~from~~ in the period between 1st of May to 31st of August 2015 (122 days). A long gap in CO₂ and H₂O flux data, due to IRGA malfunction, occurred between 25 July and 6 August 2015. Short gaps during night time amount to 737% of the total night time periods, being mainly due to limited power availability, but also low turbulence conditions. Night time was defined as the periods with PAR < 10 $\mu\text{mol m}^{-2} \text{s}^{-1}$. Other instrumental problems causing spikes in the measured CO₂ and H₂O signals (mainly caused by rain) were eliminated by the despiking method as described in Section 2.33-1 and by visual inspection of the raw data timeseries. The 30 min time series containing more than 5 spikes were discarded from further analysis, causing a loss of about 4% of CO₂ and H₂O data and 13% of sonic anemometer data. Only the 30 min records with friction velocity (u^*) larger than 0.1 m s^{-1} and fluxes with stationarity less than 1 (Foken and Wichura, 1996) were used in further analyses. Finally, the overall data coverage for quality-controlled and filtered CO₂, sensible and latent heat fluxes during the ~~selected~~ chosen period was 2835%, 338% and 356%, respectively. CO₂ nocturnal data of August was affected by spikes and so excluded from analysis.

Flux footprint was estimated using the Kormann and Meixner (2001) model. In the calculations, a value of 0.12 m (an average for May-August calculated from sonic anemometer data assuming a logarithm wind profile in near-neutral stability conditions) for the aerodynamic roughness length was used, whereas wind speed, Obukhov length and standard deviation of lateral wind velocity component were acquired from the EC data. The average source area contributing ~~to~~ 70% of the flux ranges from 89 m in unstable conditions up to about 116 m in near-neutral and 202 m in stable conditions (Fig. 1d).

2.5 Energy flux gapfilling

In order to avoid systematic bias in calculation of cumulative energy flux values, the energy flux time series were gapfilled. The soil heat flux record was complete, as for its calculation gapfilled peat temperature series were used. The rest of the fluxes were gapfilled individually following Falge et al. (2001). First, the net radiation flux was gapfilled using the mean diurnal variation (MDV) and lookup tables for longer gaps, and with linear interpolation for shorter gaps. Next, LE and H were gapfilled using linear regression against R_n . The MDV and linear regression models were calculated in a moving time window 10 days wide. The R^2 of the gapfilling models reached 0.68 for H, 0.81 for LE and 0.89 for R_n .

23.63 Partitioning and gapfilling of Net Ecosystem Exchange

The net ecosystem exchange (NEE) measured by EC was partitioned into ecosystem gross primary production (GPP) and ecosystem respiration (R_e), and then gapfilled, following the next steps:-

1) A NEE model incorporating a Q_{10} -type expression for respiration and a rectangular hyperbolic GPP expression (Eq. 6) was fit to the data at $PAR < 300 \text{ Wm}^{-2}$. The R_e -model (R_{mod}) was calculated from a Q_{10} type temperature response curve fitted to the night time EC data, when respiration is the only component of NEE. Night time was defined as all the periods when the solar elevation angle was lower than 5° . Peat temperature at a 5 cm depth was used as the driver of R_e , and the following equation

$$NEE = \underbrace{R_{ref} Q_{10}^{\left(\frac{T_0 - T_{ref}}{10}\right)}}_{a) R_e} - \underbrace{\frac{P_{max} PAR}{k + PAR}}_{b) GPP} \quad (6)$$

was fitted to the NEE data (Fig. 3a), where T_0 is the area-weighted average temperature of hollows and hummocks is the peat temperature at a 5 cm depth ($^\circ\text{C}$), T_{ref} the reference temperature of 12°C , R_{ref} the reference respiration (of $0.8 \mu\text{mol}(\text{CO}_2) \text{ m}^{-2} \text{ s}^{-1}$), and Q_{10} the temperature sensitivity, PAR the photosynthetically active radiation ($\mu\text{mol}(\text{CO}_2) \text{ m}^{-2} \text{ s}^{-1}$), P_{max} the maximum photosynthesis ($\mu\text{mol}(\text{CO}_2) \text{ m}^{-2} \text{ s}^{-1}$), k the value of PAR at $1/2P_{max}$ ($\mu\text{mol}(\text{CO}_2) \text{ m}^{-2} \text{ s}^{-1}$) of 2.3. All the four parameters (Q_{10} , R_{ref} , P_{max} and k) were evaluated by fitting at this step. The resulting $Q_{10}=1.99$ (95% CI [1.42; 2.57]) was then fixed for the whole study period.

2) The respiration module (a) of Eq. (6) was fit to the nighttime data in a 30-day-wide moving time window, with R_{ref} being evaluated at each step. The window was shifted by 1 day steps.

3) In the same time window, GPP was calculated as the residual of measured NEE and respiration model, after which the GPP module (b) of Eq. (6) was fit to produce the values of P_{max} and k .

4) The daily “window” values of R_{ref} , P_{max} and k were then smoothed out with the spline interpolation procedure and rescaled down to the 30-minute resolution of the original data. Fig. 3 shows the resulting parameter time series.

5) Finally, the R_e and GPP models were calculated at a 30-min resolution and used to fill the gaps in the measured NEE. Then, a gross primary productivity (GPP) estimate was calculated by subtracting R_e from the EC-derived NEE. In order to gap fill the GPP time series, a Michaelis-Menten type model employing photosynthetically active radiation (PAR) as a driver was used,

$$GPP_{mod} = \frac{P_{max} PAR}{k + PAR} \quad (7)$$

The fitting procedure was executed within a 30-day moving time window (Fig. 3b). The GPP model parameter values so obtained were then smoothed out with the spline interpolation procedure and rescaled down to the 30-minute resolution of the original data. Finally, the model GPP for 30-min average values of P_{max} , k and PAR was calculated from Eq. (7).

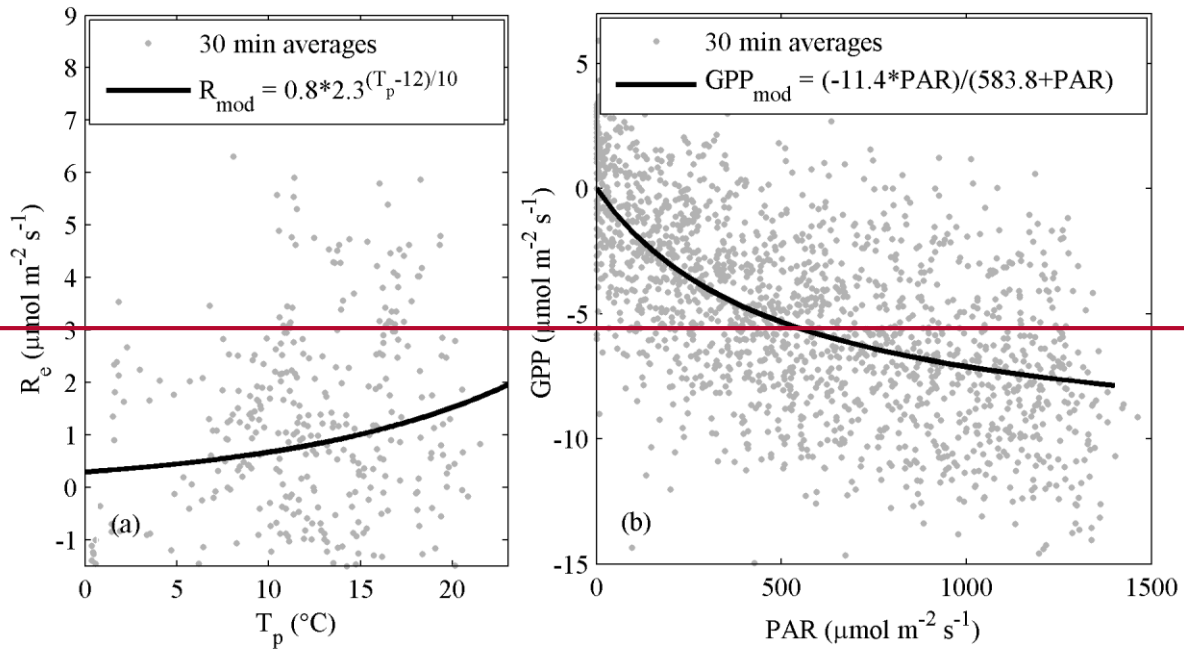
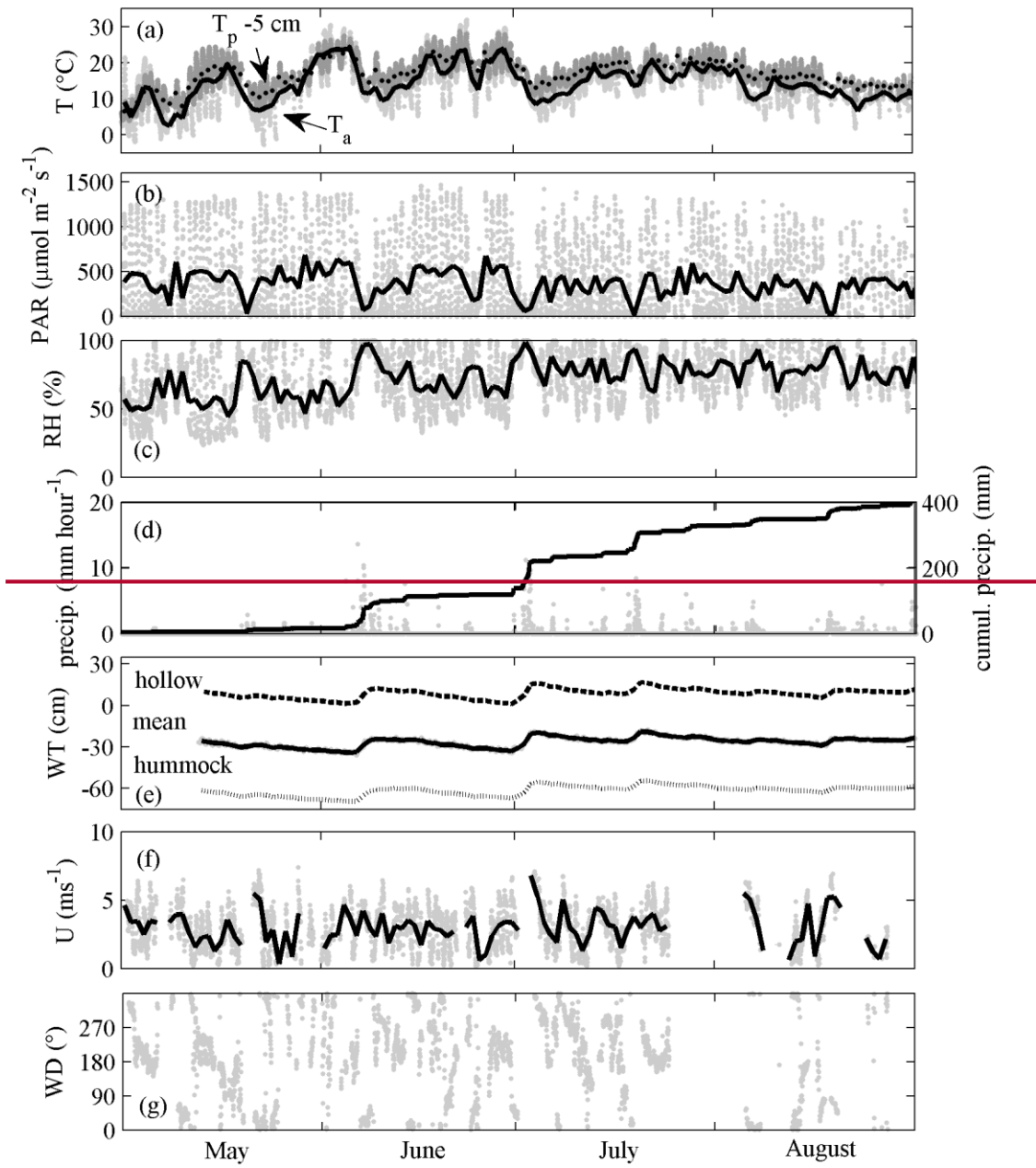


Figure 3 CO₂ flux : (a) Night time ecosystem respiration as a function of peat temperature at 5 cm depth; (b) average light response function fit to all available data.

980 **34. Results and discussion**

34.1 Environmental conditions

Air temperature Weather fluctuations in Mukhrino during the summer season of 2015 at Mukhrino were was unusual for the local-regional climate. The spring was early and warm: the average air temperatures in May and June were 4.1 $^{\circ}\text{C}$, or 3.4 $^{\circ}\text{C}$ higher than the long-term average (Fig. 34a). It caused an unusually early and rapid dramatic snowmelt- in April and the beginning of May; the last patches of snow melted by 3rd May, while three temperature profiles out of four indicated freezing until 3rd May at -5 cm and until 6th May at -20 cm depths with a further increase of peatland water table level in May-June. In contrast to the climatic average, June was the warmest month with an average air temperature of 18 $^{\circ}\text{C}$ and a maximum value of 32 $^{\circ}\text{C}$. However, the rest of summer was greatly affected by the cool fronts that brought precipitation and cloudiness. For this reason, The beginning of June was characterized by a lowered air temperature; the average July and August values sunk below the average by 2.7 and 1.7 $^{\circ}\text{C}$, respectively. In contrast to most previous years, June was the warmest month with an average air temperature of 18 $^{\circ}\text{C}$ and a maximum value of 32 $^{\circ}\text{C}$. Maximum soil temperature at a 20 cm depth (21-19 $^{\circ}\text{C}$) was observed in the last decade of June, while soil temperature at 50 cm had two maxima of 16 $^{\circ}\text{C}$ in beginning of July and in first decade of the August (Fig. 34a). Photosynthetically active radiation was at its maximum in May-June, slightly decreasing in July and August (Fig. 34cb). The maximum midday value of 1463 $\mu\text{mol m}^{-2} \text{s}^{-1}$ was registered in the middle of June.



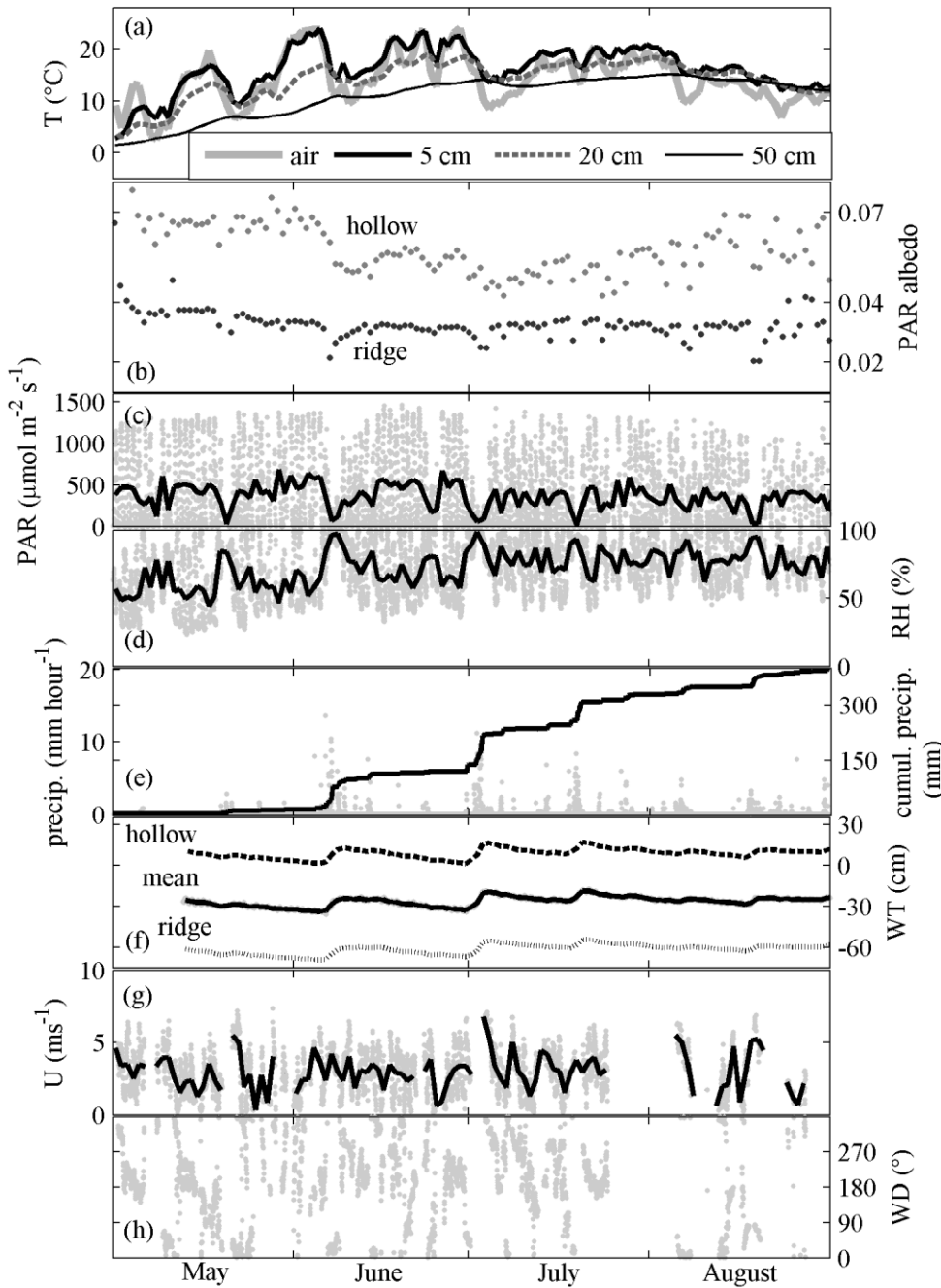


Figure 34: Time series of the environmental variables: (a) air and peat temperatures, (b) PAR albedo, (c) PAR, (d) relative humidity, (e) precipitation, (f) water table depth, (g) wind speed and (h) wind direction. The grey dots are 30 min measurements, while the black-lines lines represent daily averages, except in (b) where the dots are midday (10:00-16:00) medians of PAR albedo and in (e) where a bold line shows the cumulative precipitation. In (a), the presented peat temperatures are area-weighted averages of 2 hollow and 2 ridge measurement locations.

Precipitation considerably differed from the 81-year reference period (not shown). It was 2.7 times higher in June-July because of three heavy rainfall periods (4-9 June, 2-5 July, 18-20 July 2015). The total cumulative precipitation of the study period (May-August) was 405 mm, or 45% higher compared to the reference period, and 325 mm in May-July (Fig. 34e). The frequent precipitation helped to sustain high relative humidity (d). Accordingly, the water table depth (WTD) changes followed the intensity and frequency of precipitation, decreasing slowly during dry periods, and rapidly

1010

increasing in heavy rain (Fig. 34fe). The snow resided on the ground until ~~3rd28 May~~ April and after 30th September ~~in 2015~~. In fact, the end of snowmelt can be seen as a steep reduction in PAR albedo in the beginning of May (Fig. 4b; the hollow albedo starts at 0.12 in early May, but the axis is limited at 0.08 for clarity). Otherwise, PAR albedo follows the typical trends, being higher in the hollows than in the ridges and showing downward peaks during the precipitation events.

1015

The prevailing wind direction was from the South/South-West (150-260°, 45% of cases), in which the proportions of open water, hollows and ridges within the 200 m radius are 1%, 67% and 32%, correspondingly. ~~Similar~~ The same proportions hold for the entire area within ~~the a~~ 200 m radius around the mast, ~~implying high anisotropy of surface types~~.

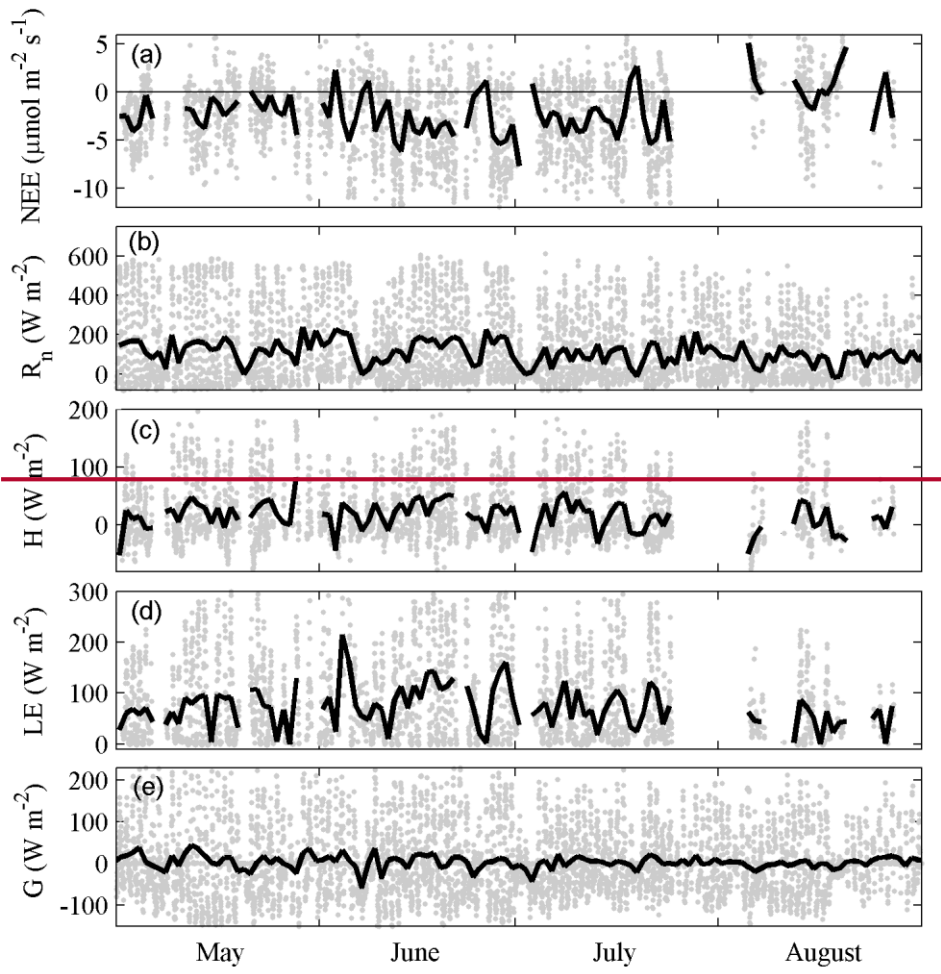
1020

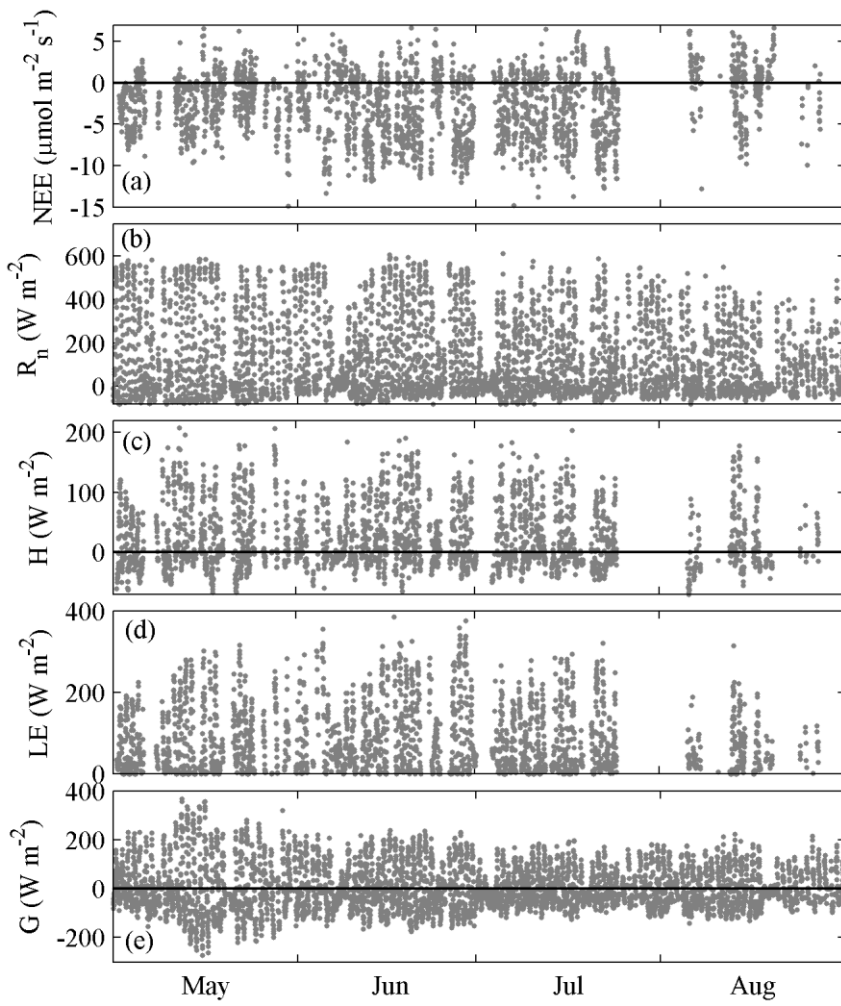
34.2 Surface energy exchange

Time series of the surface energy fluxes and their monthly diurnal courses are shown in Figs. ~~45 and -56~~, respectively. The midday net radiation (R_n) averaged 397 $W m^{-2}$ and 364 $W m^{-2}$ in May and June, respectively, reflecting the large amounts of incoming solar radiation (Fig. 3c4). However, the high post-snowmelt water levels and undeveloped vascular vegetation in May resulted in low albedo, somewhat lowering R_n . On the other hand, the midday values in the second part of the summer are clearly lower, being 275 $W m^{-2}$ and 211 $W m^{-2}$ in July and August, respectively. In fact, as later in the summer the developed ground vegetation attains a higher reflectivity, this increases the surface albedo and decreases R_n . In addition, ~~because of slightly larger number of the frequent~~ overcast ~~conditions~~ days (~~16 days in July and 17 in August~~) ~~further reduced~~, the amount of incoming solar radiation ~~is lower in late summer compared with May and July~~ (Table 1). The soil gained heat throughout most of the studied period, but the average flux is very small, ranging from 8 $W m^{-2}$ in May to 1 $W m^{-2}$ in July. The ground starts to cool down in August with G equaling -4 $W m^{-2}$.

1025

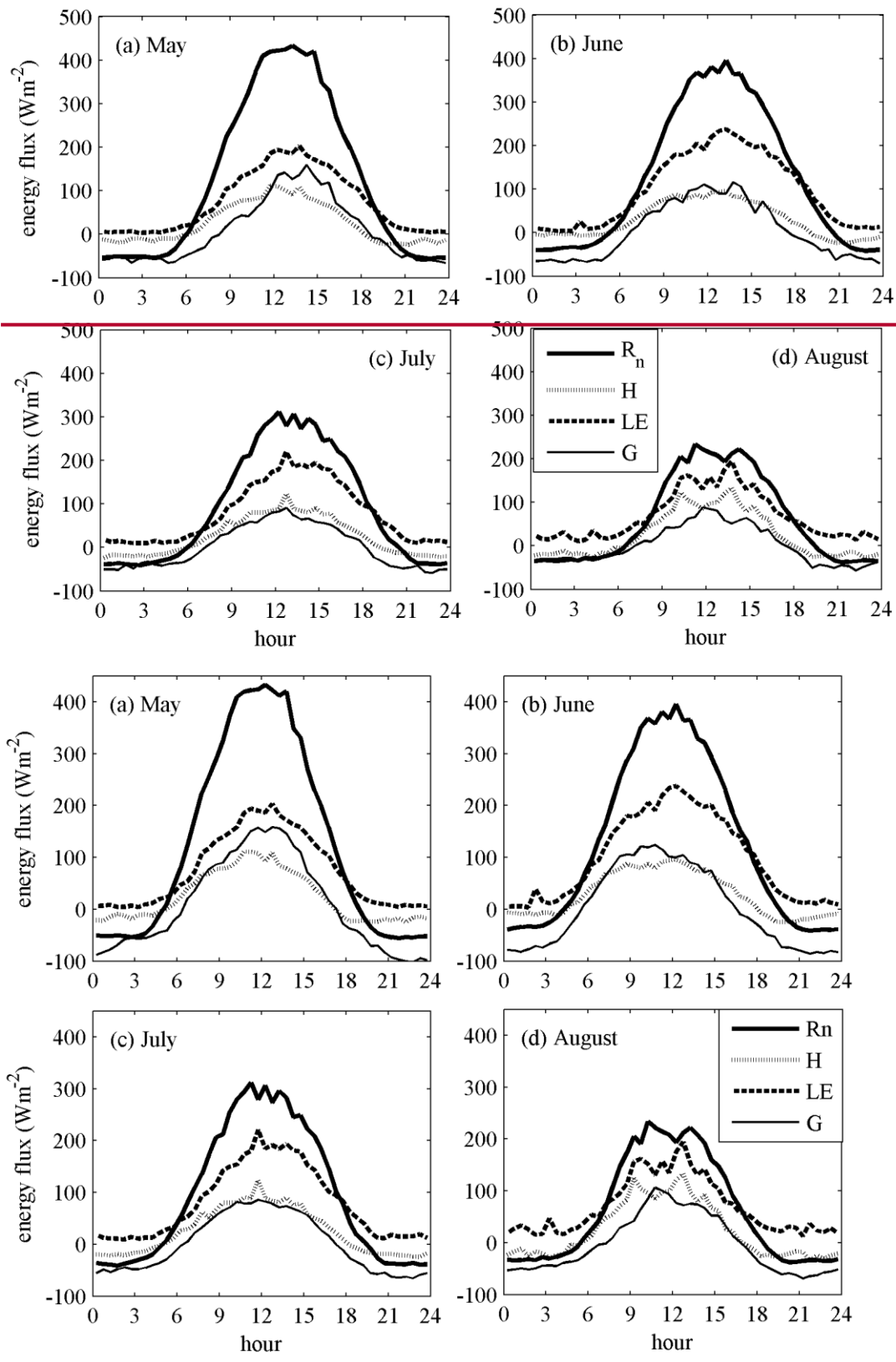
1030 Most of the available energy is released as latent heat flux, whose monthly average values are between 61 and 96 $W m^{-2}$, while sensible heat fluxes are more than three times lower ranging from 30 $W m^{-2}$ in July to 13 $W m^{-2}$ in August (Table 1).





1035

Figure 45: Time series of the 30-minute average surface fluxes measured with the eddy-covariance system: (a) net ecosystem exchange, (b) net radiation, (c) sensible heat, (d) latent heat, and (e) ground heat flux. The grey dots are 30 min measurements, while the black line represents daily averages.



1040 **Figure 56:** Monthly average diurnal courses of the energy balance components. The time shown in the x-axis is local winter time (UTC+5).

1045

There is a ~~clear-marked~~ seasonal change in LE, which starts to increase rapidly in May due to high R_n values, reaching the daily mean peak in July (239 W m^{-2}), and then decreases in July reaching the minimum value at noon of about 140 W m^{-2} in August (Fig. 5 and Table 1).

1050

Table 1. Monthly averages of air temperature (T_a), soil temperature at 5 cm depth (T_p), photosynthetic active radiation (PAR), cumulative precipitation (mm), net radiation (R_n), ground heat flux (G), sensible heat flux (H), latent heat flux (LE), Bowen ratio (β), energy balance residual ($\text{Res} = R_n - H - \text{LE} - G$), energy balance closure ($\text{EBC} = (H + \text{LE} + G) / (R_n)$), and gapfilled NEE.

	T_a [°C]	T_p [°C]	PAR [Wm^{-2}]	P [mm]	WTD [cm]	R_n [Wm^{-2}]	G [Wm^{-2}]	H [Wm^{-2}]	LE [Wm^{-2}]	β [-]	Res [Wm^{-2}]	EBC [-] [%]	NEE _{gapf} [gC m^{-2}]
May	11.1 11.1	11.8 10.1	405399 0	1242. 2	-17- 28.6	126429 -6	87.6 87.6	2323.2 2323.2	7374.5 7374.5	0.32 0.31	2218.8 2218.8	7 7	-35-35 -35-35
June	17.9 18.0	19.6 18.1	411403 9	1214 21.2	-16- 28.5	133428 -6	33.3 33.3	3030.3 3030.3	96400. 96400.	0.27 0.30	5-7.1 5-7.1	05 05	-72-68 -72-68
July	15.2 15.0	18.0 16.9	318324 1	1914 91.4	-11- 22.7	8892.6 14.3	14.3 1522.7	1522.7 1522.7	6975.5 6975.5	0.27 0.30	3-2.2 3-2.2	02 02	-79-77 -79-77
August	12.6 12.6	15.2 13.4	295247 1	8080. 0	-13- 26.7	6275.9 -40.7	-40.7 1316.4	1316.4 1316.4	6159.8 6159.8	0.26 0.27	-8-20.6 -8-20.6	29 29	-16-15 -16-15
May- August	14.3 14.3	16.1 14.6	359342 3	4054 04.8	-14- 26.4	102407 -7	102407 23.2	2024.7 2024.7	7481.7 7481.7	0.28 0.30	60.8 60.8	9 9	-202-196 -202-196

1055

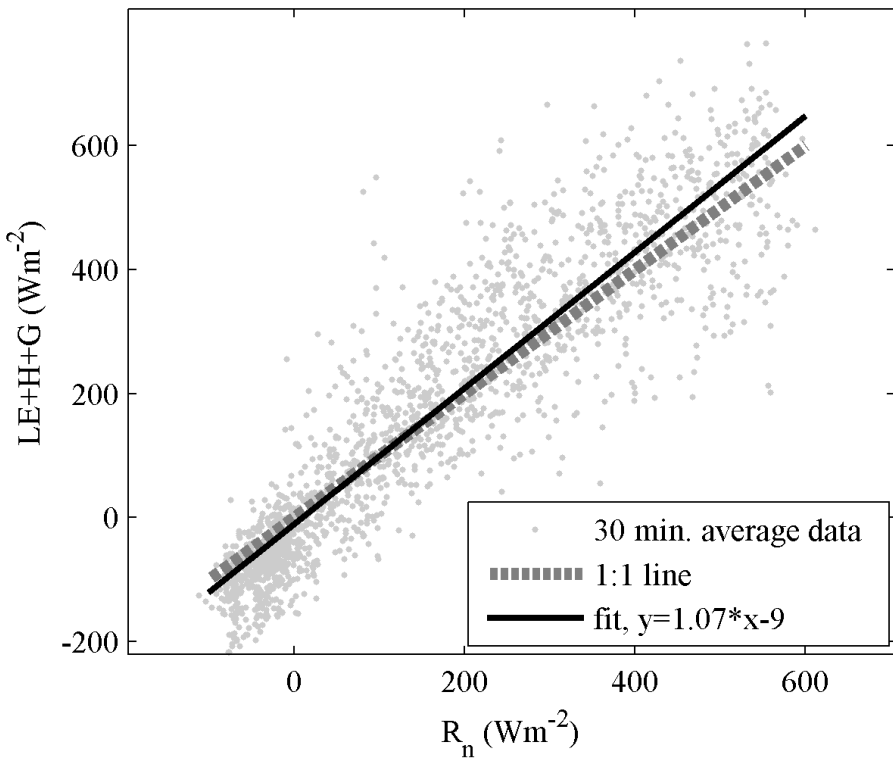
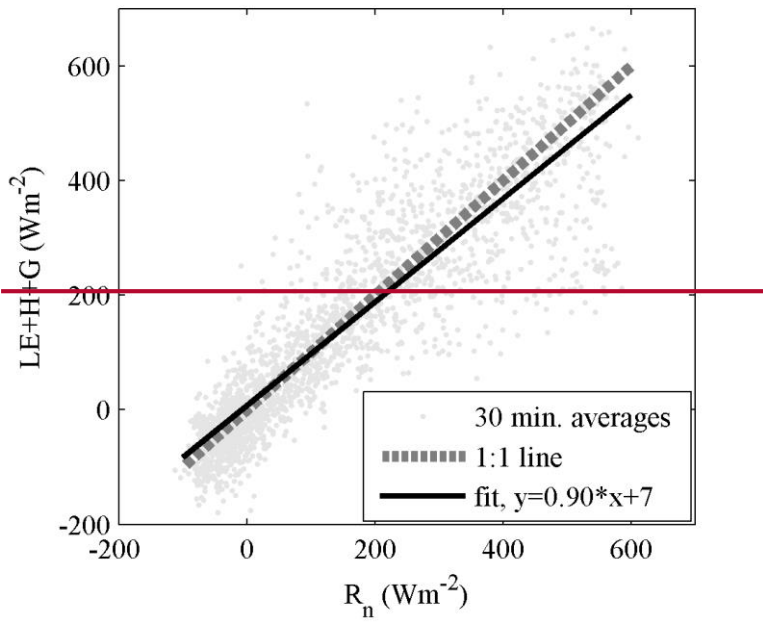
1060

1065

Although a seasonal change of H is also observed, it is characterized by a smaller amplitude. Monthly mean values of Bowen ratio (β) are rather low (around 0.3), showing no significant seasonal variation (Table 1). However, the sequence of rainy and ~~sunny-dry~~ periods caused short-term variations of β between 0.15 and 0.6 ~~with-on~~ a timescale of about 2 weeks. Turbulent heat fluxes (H and LE) show a diurnal variation typical of land ecosystems, being in phase with R_n (Fig. 56). The dominance of LE (with respect to H) for northern wetlands has been already reported. Using a flux tower in a Western Siberia bog site located close to Plotnikovo ($56^{\circ}51' \text{ N}$, $82^{\circ}50' \text{ E}$), Shimoyama et al. (2003) show values of β ranging from 0.57 in the early growing season to 0.78 in the peak growing season. Similar values were found by Aurela et al. (2015) in a Finnish wetland ($\beta = 0.78$, Lompolojankkä) and in the wetland site Degerö in Sweden ($\beta = 0.83$, Peichl et al. (2013)). However, lower values of β , more similar to the one in our study, were observed in other northern wetlands (Runkle et al., 2014; Wu et al., 2010; Eugster et al., 2000). Most probably, the difference can be explained by difference in water table depths. One has to account also for the unusually wet conditions in 2015 ~~when the measurements were made~~, which must have enhanced LE to a certain extent. High water availability supported high LE and G in May and June. The subsequent reduction in G could have been partly related to higher ground shading by aboveground biomass.

The energy balance closure (EBC) for the whole period is around 1.0790% (Fig. 67) when adopted as a slope of $\text{LE} + \text{H} + \text{G}$ vs. R_n , or 0.99 when calculated as a ratio of the corresponding cumulative fluxes. The slight excess on the side of $\text{H} + \text{LE} + \text{G}$ might be the product of uncertainty in the modeled peat water content (Eq. 5), which may in turn have affected G. Monthly estimates of the EBC and the residual (Res) are reported in Table 1. The EBC (ratio method)

1070 ranges from ~~0.8787%~~ in May, when the difference between available energy and the turbulent fluxes is ~~+8.822~~ W m⁻²,
to ~~+291.27%~~ in August, when Res is ~~-820.6~~ W m⁻². The summer months (June and July) show the best values of EBC
and Res. The observed values are in line with those from other wetland studies (Kurbatova et al., 2002; Peichl et al.,
2013; Runkle et al., 2014). In their FLUXNET site--based energy balance closure study, Stoy et al. (2013) reported an
1075 average value of 0.76 for the wetland site category, highlighting the relevance of including the heat storage term in sites
with high water table depth. Shimoyama et al. (2003) obtained a better EBC value (0.9 vs 0.82 in July), estimating the
soil heat flux in the bog from an area--averaged value of soil thermal parameter (instead of using a point value),
~~somehow to some extent~~ accounting for the surface heterogeneity and the presence of microtopography. Our use of
area-weighted average temperature profiles and individual water level measurements in the ridge ~~The low value of~~
~~EBC observed in May in Mukhrino probably stems from the high degree of spatial heterogeneity (with part of the~~
1080 ~~ground covered by water), producing high uncertainty in the estimated G. On the other hand, the highest residual found~~
~~in August (-20.6 W m⁻²) is mainly due to low data coverage for this month. and hollow microsites has resulted in a~~
similarly high EBC, implying that the main component of spatial heterogeneity must have been captured.



1085 **Figure 67:** Energy balance plot. The sum of latent and sensible heat fluxes and soil heat flux is plotted against net radiation flux. A linear function is fit to the data and shown together with a 1:1 line. The mean ratio of $(LE+H+G)$ to R_n is 0.99.

1090

34.3 Net Ecosystem Carbon Exchange

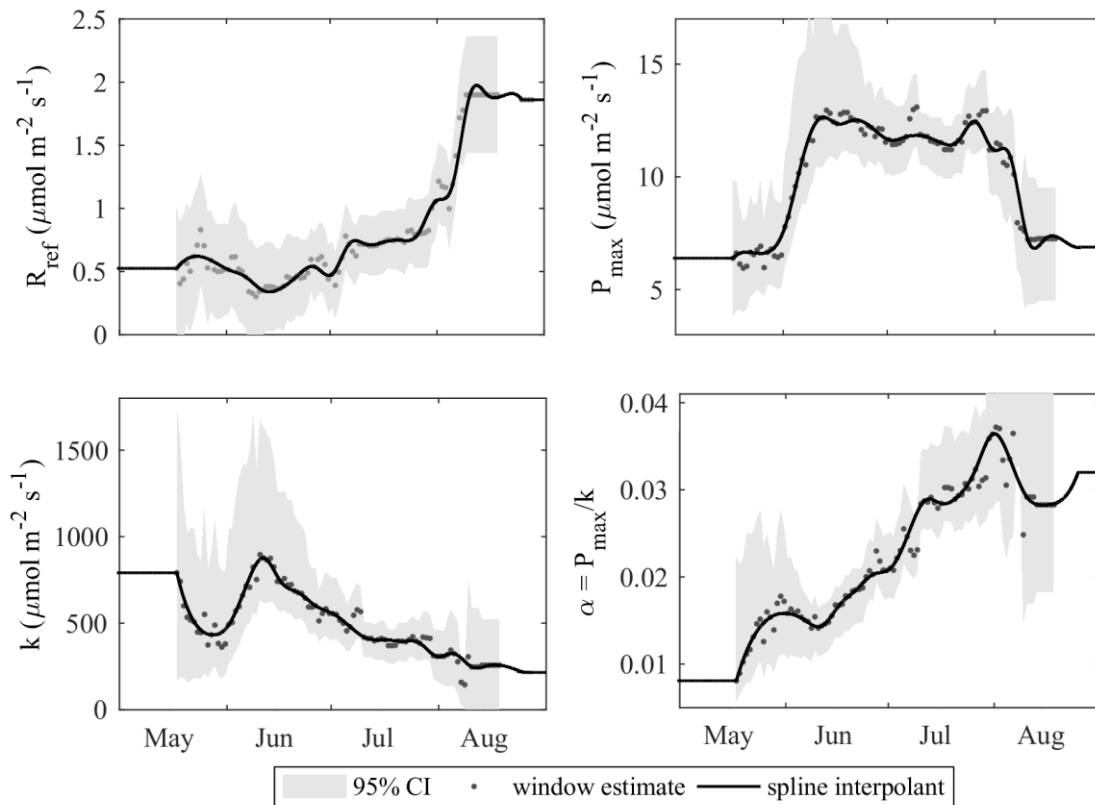


Figure 7: time series of the CO₂ flux model parameters. The dots are the daily values evaluated in a moving time window, and the solid line is a spline-interpolant, while the shaded area shows the 95% confidence interval, which is calculated at each time window step. The interpolated parameter lines stretch to the beginning of May and end of August, showing the constant values used on the edges of the study period.

The time series of P_{\max} , k , quantum yield α and R_{ref} presented in Fig. 7 reveal notable trends. R_{ref} drops between May and early June, possibly related to rainy weather spells, but then increases rapidly by August, probably in response to the increasing soil temperatures, availability of substrate and plant productivity. P_{\max} has a broad peak in June-July, which is probably governed by the vascular leaf area index, with a possible contribution of the acclimation, as the air temperatures were closer to optimal in that period (see Fig. 10 below). k had a maximum in June, with a later gentle reduction towards August. This evidence of higher photosynthetic activity at low light in late summer may again point at acclimation. In turn, the P_{\max} and k evolutions result in a May-August upward trend in α . However, one could speculate that this behavior is due to the seasonality of plant functional group activity, to an extent. A Finnish boreal fen study of Korrensalo et al. (2017) found a wide seasonal variation in the contributions of moss and vascular species to the ecosystem-scale photosynthesis. The moss photosynthesis ($\text{gC m}^{-2} \text{d}^{-1}$) declined steadily throughout summer, while various vascular species were most active in June, July or August; it was also common for k of many species to have a peak in June and/or become reduced throughout the growing season, in line with the findings of the current study.

The time-series of ~~measured-gapfilled~~ NEE is shown in Fig. 8a. The largest flux amplitudes are found during June and July when half-hour values range between ~~about~~ $-10 \mu\text{mol m}^{-2} \text{s}^{-1}$ and $5 \mu\text{mol m}^{-2} \text{s}^{-1}$. In May, the measured NEE has a narrower amplitude because of lower temperature and PAR values. Monthly differences in the NEE amplitude can be clearly seen in Fig. 9, where the mean diurnal course is plotted for each month. The modelled NEE, ~~calculated as~~ $(R_e - \text{GPP})$ (Eq. 6), ~~closely~~ follows ~~very closely~~ the measured NEE ~~in each month, except in August when R_e is~~

1115 ~~underestimated~~. As expected, the largest net carbon uptake was observed in June and July (~~-72~~ and ~~-79~~ gC m⁻²,
respectively), while in May it amounted to ~~-35~~ gC m⁻². Unfortunately, poor data coverage was achieved in August,
making the corresponding monthly cumulative value somewhat more uncertain, although it seems to have been much
lower (~~-16~~ gC m⁻²). Overall, the bog site acted as a net CO₂ sink in the analyzed period. The cumulative gap-filled NEE
for of May-August was ~~-202~~ gC m⁻², which decomposes into ~~462-157~~ gC m⁻² of R_e and ~~-358-364~~ gC m⁻² of GPP. For the
1120 period of May-July ~~having-with~~ the best data coverage, the corresponding values were ~~-184-186~~, ~~127-91~~ and ~~-308-277~~
gC m⁻². ~~The Mukhrino May-August GPP falls between 224-243 gC m⁻² observed over the same period by two Canadian
bogs and 466-539 gC m⁻² in Mer Bleue (Humphreys et al. (2014)).~~ However, in terms of net summer uptake, the
~~Mukhrino observed in Mukhrino~~ was among the highest estimates. For example, Friborg et al. (2003) reported an
average ~~July~~ CO₂ uptake of -7545 mg m⁻² d⁻¹ (which corresponds to a cumulative sum of -64 g C m⁻²) measured ~~in July~~
1125 ~~bywith~~ EC ~~system located~~ at the Bakchar bog close to Plotnikovo village in West Siberia. This value is very close to the
Mukhrino NEE sum of June (Table 1). Lower CO₂ uptake is reported for Zotino bog, where growing season (May-
October) cumulative NEEs range between -43 and -60 g C m⁻² in different years, with maximum daily mean NEE of
about -2 μmol m⁻² s⁻¹ measured in July 2000 (Arneeth et al., 2002). ~~A similar-Lower~~ NEEs in the range of -50 to -90 gC
m⁻² year⁻¹ ~~were~~ shown ~~by-for~~ several peatlands of Northern European Russia and Siberia (Dolman et al., 2012). Daily
1130 net carbon uptakes ranging between -1 and -2.8 g C m⁻² d⁻¹ were measured during summer in other northern peatlands in
Canada (Humphreys et al., 2006); ~~compare with the June-August average of -1.8 g C m⁻² d⁻¹ in Mukhrino.~~

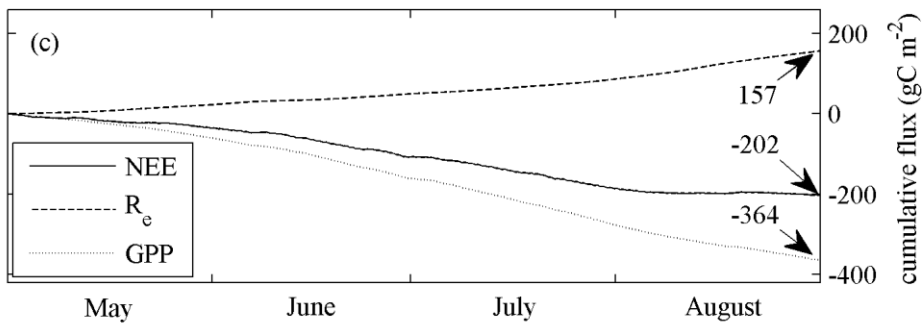
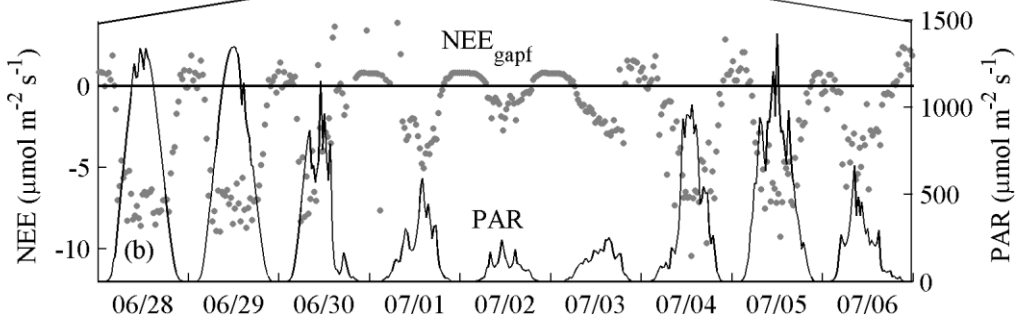
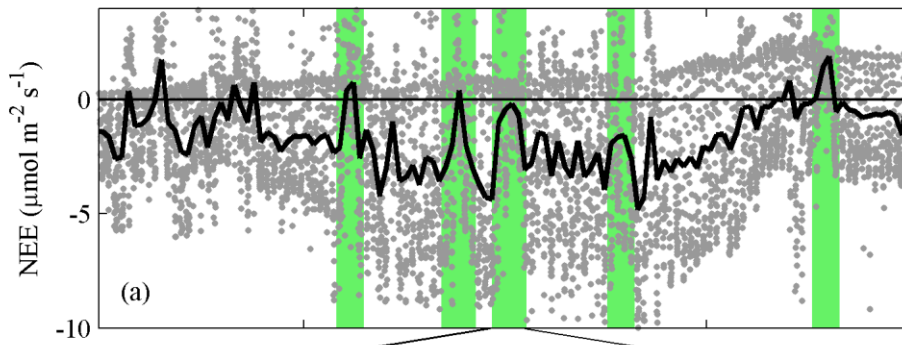
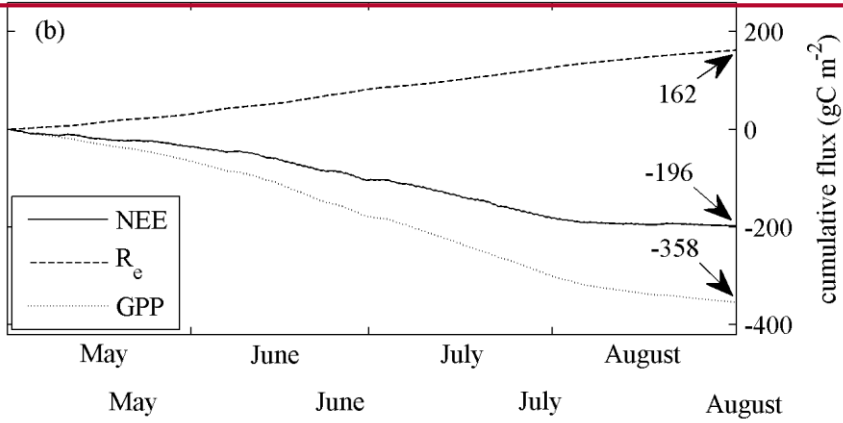
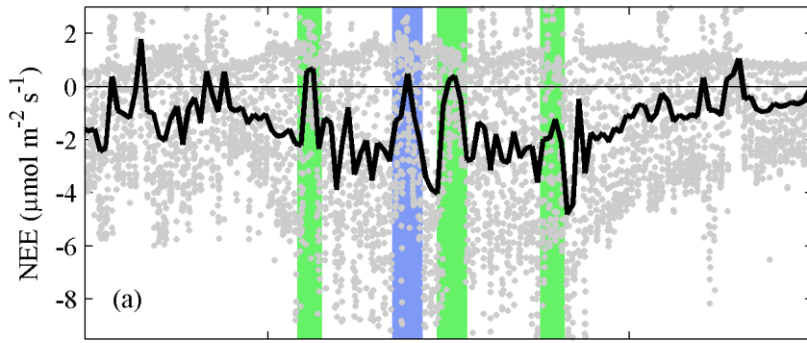
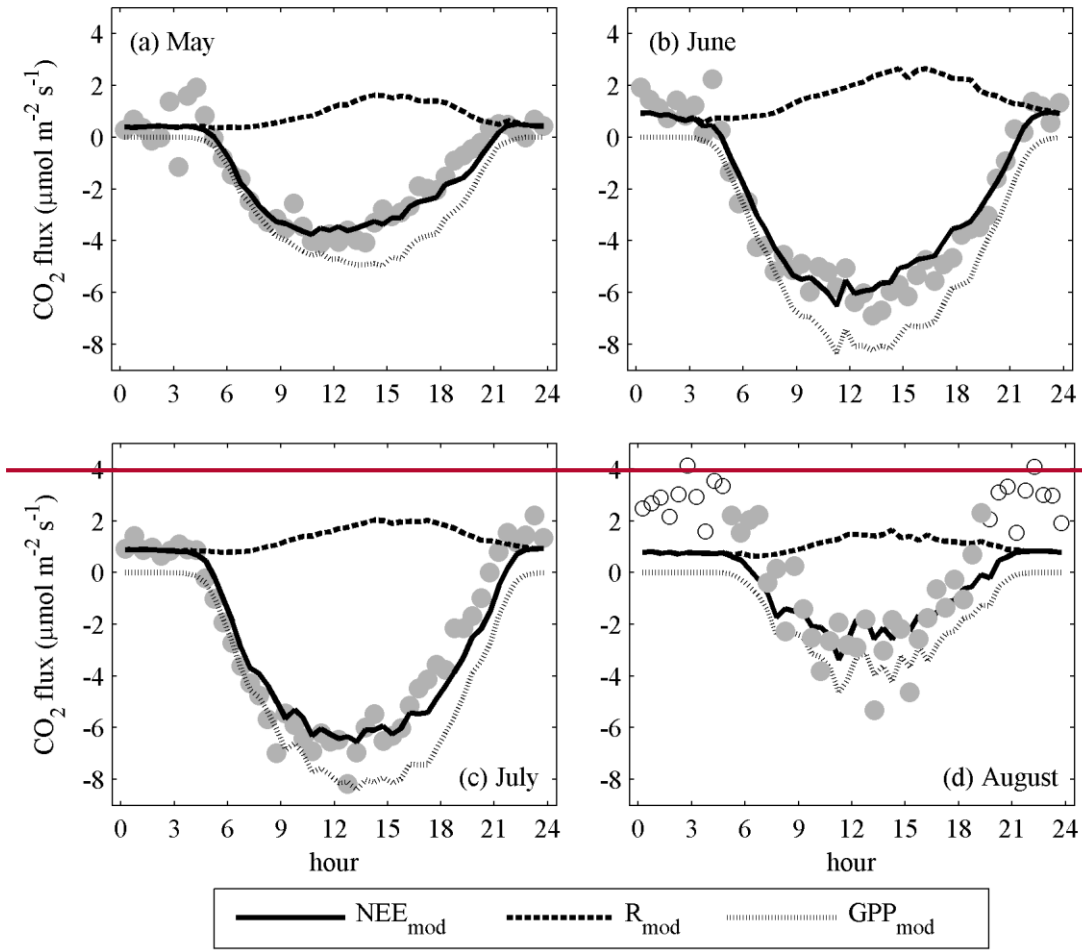
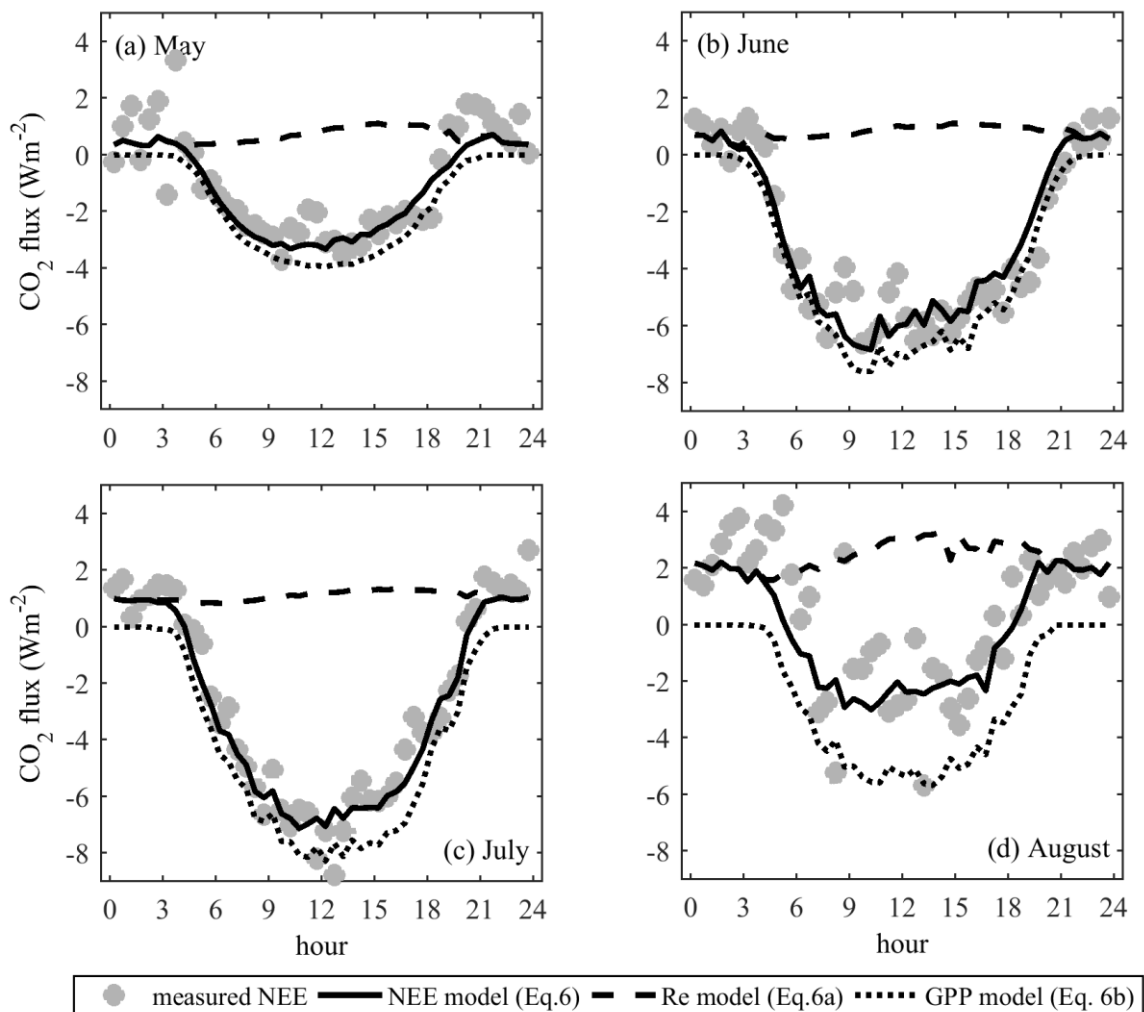


Figure 8: (a) Seasonal variation of NEE measured with the eddy-covariance system; the grey dots correspond to 30 min averages and the black line to the daily averages. The major rainy-fronts passage events are marked with green ~~and the rain-free front with blue.~~ (b) Measured NEE and PAR during the third frontal event. (c) Cumulative gapfilled NEE, R_e and GPP.





1140 **Figure 9:** Mean diurnal course of NEE and its components for individual months during the study period. The time in
 1145 the x-axis corresponds to local winter time (UTC+5).

34.4 The effect of weather conditions

1145 The year 2015 was characterized by diverse weather, starting with an early and warm spring and continuing rainy and overcast wet and cool in West Siberia. Carbon uptake became significantly limited during the passage of four-five cold fronts that occurred in June--and August/July (see Fig. 8), three-four of which were associated with ample precipitation. During those short periods, uptake plunged to very low values, with the ecosystem even becoming a net-CO₂-neutral or a small source during the first three rainy-some periods. A closer look at one such period is provided by Fig. 8b. Excluding the rain-free front in late June, each event brought about 100 mm of precipitation, causing WT raises of 8-11 cm (Fig. 3-4 d,e). However, no dependency of surface exchange on WT was found. The regular and ample precipitation helped sustain water level at a nearly constant level, which was about -60 cm in ridges, while many hollows stayed inundated (Fig. 3f). In a landscape dominated by ridges (in terms of green biomass), drawdown in WT leads to its decoupling from the hydrological state of surface peat (Price et al., 2003), and, therefore, all vegetation functions including photosynthesis. Sustaining high water level must prevent water stress in the hummock vegetation, which constitutes a significant fraction of green biomass in Mukhrino. In such exceptionally wet conditions as in 2015, the top peat must have stayed moisturized most of the time, meaning that water availability was not the limiting factor for CO₂

1150

1155

uptake. At the same time, the hollows stayed largely inundated and as such probably made a smaller contribution to photosynthesis than hummocks.

1160 The overcast conditions during front passage also resulted in temperature drops by up to 13 °C-degrees. This obviously limited respiration, but also restricted photosynthesis as the optimum growth temperature seems to be close to 30 °C (Fig. 10b).

~~In contrast, between the fronts, air temperatures did occasionally exceed 25 °C periodically, promoting photosynthesis. This behavior reflects the temperature control on GPP that is common for the whole Boreal region (Reichstein et al., 2007).~~

1165 High relative humidity, and thus lower VPD, must have partly compensated for the lower CO₂ uptake during the fronts by promoting higher stomatal conductance (g_s). In terms of the parameters g_1 and m (Fig. 10a), the response of g_s to VPD was similar to that in southern Swedish bog Fäjemyr, northern Swedish fen Degerö and southern Finnish fen Siikaneva (Alekseychik et al., unpublished data; Peichl et al., 2013). Mean bulk surface resistance (r_s , the reciprocal of conductance) of 74 s m⁻¹ is somewhat lower than approximately 85 s m⁻¹ reported for the “wetlands” ecosystem class by (Kasurinen et al., 2014). As mentioned above, the Bowen ratio was stable throughout the summer (~0.3), but the weekly mean values varied between 0.152 and 0.6 in close correlation with the precipitation and cloudiness pattern.

1175 Nevertheless, the favorable conditions of May and early June allowed for apparent rapid accumulation of green biomass. In Also, contrast, between the cold fronts, air temperatures did occasionally exceed 25 °C periodically, promoting photosynthesis. This behavior reflects the temperature control on GPP that is common for the whole Boreal region (Reichstein et al., 2007). As a result, the early spring and sustained wetness for the rest of the year seem to have outweighed the GPP restriction during the front passages, and eventually led to an unusually high cumulative CO₂ uptake.

1180 No flux variation with wind direction was found, in consistency with the the-similarity of ridge-hollows fractions in different wind direction sectors high homogeneity of the landscape within the EC footprint (Fig. 1 c₂-d).

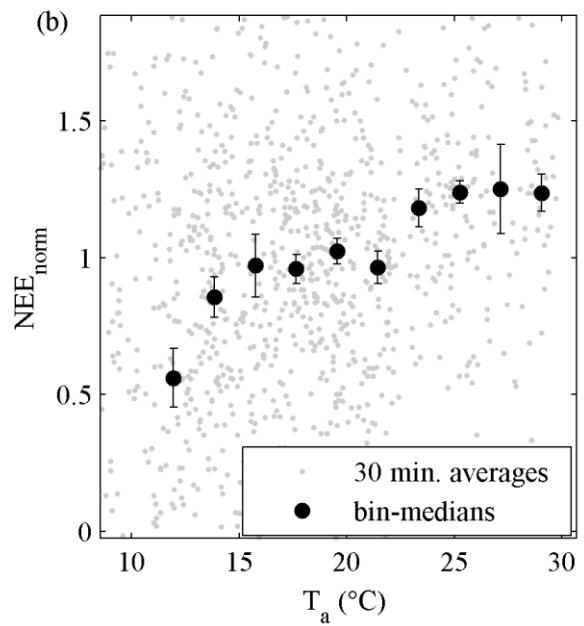
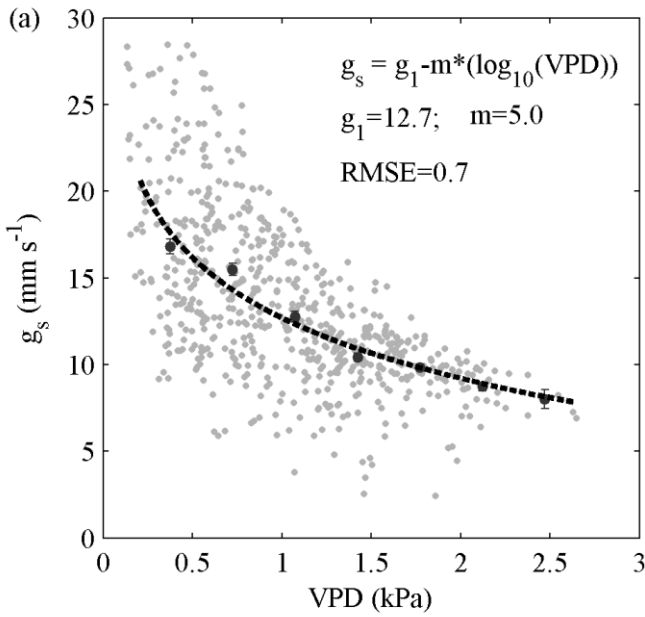
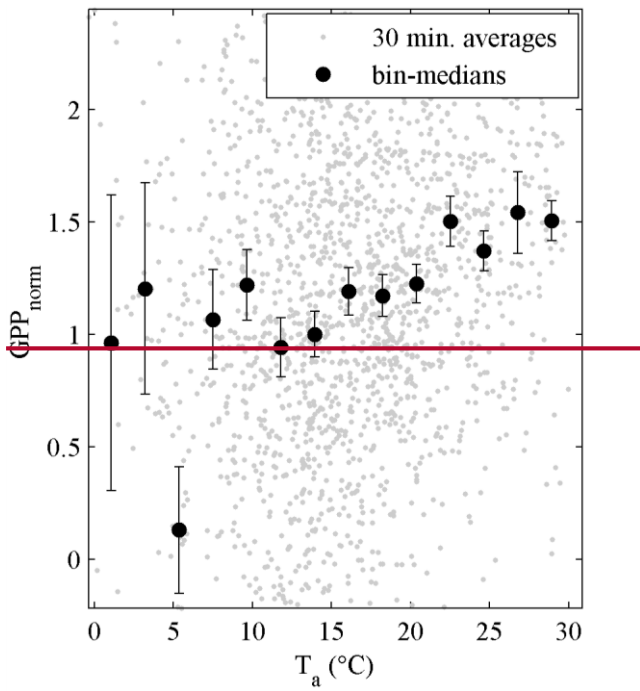


Figure 10: (a) Surface conductance *versus* vapor pressure deficit demonstrating a well-known relationship. The dashed line is a fit (the function is specified in the insert). (b) Normalized NEE ($NEE_{norm} = \frac{GPP - NEE}{GPP}$) *versus* air temperature for June-July 2015 normalized by its model *versus* air temperature. The grey dots are the 30 min average data, and the black circles with error bars the bin medians. NEE_{norm} saturates approaching 25 °C.

1185

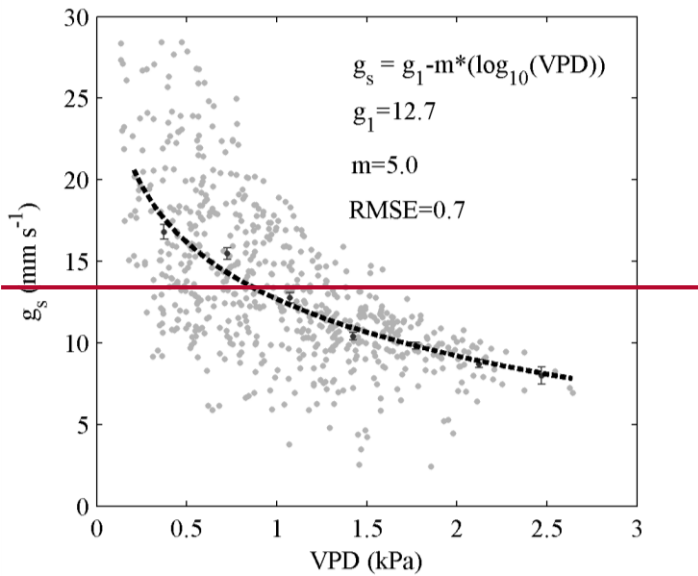


Figure 11: Surface conductance versus vapor pressure deficit demonstrating a well known relationship. The grey dots are the 30 min average data, black dots with error bars the bin averages, and the dashed line the fit (the function is specified in the insert).

4.5. Conclusions

This study provides the results of direct and continuous measurements of surface energy balance components and CO₂ flux at the Mukhrino bog site in West Siberian middle taiga. The turbulent fluxes measured by the EC technique over May-August 2015 represent form the a pioneering dataset of its kind for the region.

The observed magnitudes and diurnal course of sensible and latent heat fluxes were generally in agreement with previous bog studies. The latent heat flux was about three times larger than the sensible heat, and the monthly mean Bowen ratio did not show any significant seasonal variation. However, short-term variations related to heavy rainfall events were observed. In terms of monthly averages, May and June were characterized with the highest available energy.

Carbon dioxide exchange was typical of a raised bog, with net CO₂ sink being rather high (202 gC m⁻² for May-August) but within the range of previous observations (IPCC, 2014, 2013). Remarkably wet weather of 2015 ensured high moisture availability and thus promoted high photosynthesis during the sunny periods. However, the rainy and cool conditions during the passage of several fronts limited photosynthesis so that the ecosystem temporarily turned into net CO₂ source. The peak in carbon uptake lagged the maximum available energy by one month, falling on June-July, probably being modulated by the course of vascular plant leaf area development.

The sharp seasonality of the photosynthesis and respiration model parameters pointed at an ensemble of effect, including the variability in green biomass, which was not measured during the study period relative importance of plant functional groups, and acclimation. Complementary chamber and plant-scale studies will help disentangle those effects.

The Mukhrino station was established for the purpose of long term monitoring of ecosystem functioning and greenhouse gas exchange and continued its operation in 2016. Obtaining a measurement record over several years with varying weather would be instrumental for determining the typical budgets of the ecosystem, unaffected by untypical weather, which was the case in 2015.

Author contributions

1220 P. Alekseychik analyzed the data, produced the figures and contributed to the text. I. Mammarella wrote a major part of the text. D. Karpov and S. Dengel set up the eddy-covariance measurements, provided technical support and contributed to the text. I. Terentieva, A. Sabrekov and M. Glagolev participated in the writing process. E. Lapshina supervised the Mukhrino field station.

Acknowledgements

1225 The study was supported by INTERACT project GHG-FLUX, EU-project GHG-LAKE (project no. 612642), Nordic Centre of Excellence DEFROST, National Centre of Excellence (272041), ICOS-FINLAND (281255) and CarLAC (281196), funded by the Academy of Finland, and the Russian Foundation for Basic Research grant №15-05-07622. [We gratefully acknowledge Dr. Pasi Kolari for the valuable advice he provided.](#) The help in the field and provision of data by Yaroslav Solomin and Prof. Martin Heimann is gratefully acknowledged. Nina Filippova compiled the meteorological data. The codes and data used in this study are available upon request.

References

- 1235 Alekseychik, P., Lappalainen, H., Petäjä, T., Zaitseva, N., Heimann, M., Laurila, T., Lihavainen, H., Eija, E., Arshinov, M., Shevchenko, V., Makshtas, A., Dubtsov, S., Mikhailov, E., Lapshina, E., Kirpotin, S., Kurbatova, Y., Ding, A., Guo, H., Park, S., Lavric, J., Reum, F., Panov, A., Prokushkin, A., and Kulmala, M.: Ground-based station network in arctic and subarctic eurasia: an overview, *Geogr. Environ. Sustain.*, 9, 75-88, 10.15356/2071-9388_02v09_2016_06, 2016.
- 1240 Arneth, A., Kurbatova, J., Kolle, O., Shibistova, O. B., Lloyd, J., Vygodskaya, N. N., and Schulze, E.-D.: Comparative ecosystem-atmosphere exchange of energy and mass in a European Russian and a central Siberian bog II. Interseasonal and interannual variability of CO₂ fluxes, *54*, 10.3402/tellusb.v54i5.16684, 2002.
- Aurela, M.: The timing of snow melt controls the annual CO₂ balance in a subarctic fen, *Geophys. Res. Lett.*, 31, 10.1029/2004gl020315, 2004.
- Aurela, M., Lohila, A., Tuovinen, J.-P., Hatakka, J., Penttila, T., and Laurila, T.: Carbon dioxide and energy flux measurements in four northern-boreal ecosystems at Pallas, *Boreal Environ. Res.*, 20, 455-473, 2015.
- 1245 Belova, S.E., Oshkin, I.Yu., Glagolev, M.V., Lapshina, E.D., Maksyutov, Sh.Sh., Dedysh, S.N.: Methanotrophic Bacteria in Cold Seeps of the Floodplains of Northern Rivers, *Microbiology*, 82, 743-750, 2013.
- Bleuten, W., and Filippov, I.: Hydrology of mire ecosystems in central West Siberia: the Mukhrino Field Station, *Transactions of UNESCO department of Yugorsky State University "Dynamics of environment and global climate change"/Glagolev MV, Lapshina ED (eds.)*. Novosibirsk: NSU, 208-224, 2008.
- 1250 Bubier, J. L., Bhatia, G., Moore, T. R., Roulet, N. T., and Lafleur, P. M.: Spatial and temporal variability in growing-season net ecosystem carbon dioxide exchange at a large peatland in Ontario, Canada, *Ecosystems*, 6, 353-367, 2003.
- Bulatov, V. I. E.: Geography and ecology of Khanty-Mansiysk and its natural surroundings (In Russian) (География и экология города Ханты-Мансийска и его природного окружения), "Informatsionno-Izdatel'skiy Tsentr", Khanty-Mansiysk, Russia, 187 pp., 2007.

- 1255 Burba, G., McDermitt, D., Grelle, A., Anderson, D., and Xu, L.: Addressing the influence of instrument surface heat exchange on the measurements of CO₂ flux from open-path gas analyzers. *Global Change Biology*, 14(8): 1854-1876, 2008.
- Dolman, A. J., Shvidenko, A., Schepaschenko, D., Ciais, P., Tchebakova, N., Chen, T., van der Molen, M. K., Belelli Marchesini, L., Maximov, T. C., Maksyutov, S., and Schulze, E. D.: An estimate of the terrestrial carbon budget of
1260 Russia using inventory-based, eddy covariance and inversion methods, *Biogeosciences*, 9, 5323-5340, 10.5194/bg-9-5323-2012, 2012.
- Eugster, W., Rouse, W. R., Pielke Sr, R. A., McFadden, J. P., Baldocchi, D. D., Kittel, T. G. F., Chapin, F. S., Liston, G. E., Vidale, P. L., Vaganov, E., and Chambers, S.: Land-atmosphere energy exchange in Arctic tundra and boreal forest: available data and feedbacks to climate, *Glob. Change Biol.*, 6, 84-115, 10.1046/j.1365-2486.2000.06015.x,
1265 2000.
- Filippova, N. V., Bulyonkova, T. M., and Lapshina, E. D.: Fleshy fungi forays in the vicinities of the YSU Mukhrino field station (Western Siberia), *Environ. Dyn. Glob. Clim. Change*, 6, 2015.
- Foken, T. and Wichura, B.: Tools for quality assessment of surface-based flux measurements, *Agric. Forest Meteorol.* 78, 83-105, 1996.
- 1270 Friborg, T., Soegaard, H., Christensen, T. R., Lloyd, C. R., and Panikov, N. S.: Siberian wetlands: Where a sink is a source, *Geo. Res. Lett.*, 30, 10.1029/2003GL017797, 2003.
- Gazovic, M., Kutzbach, L., Schneider, J., Wille, C. a., & Wilmking, M. (2010). Ecological analysis of a boreal peatland CO₂ flux based on eddy covariance data set from Ust Pojog, Russia. In EGU General Assembly Conference Abstracts (pp. 10049).
- 1275 Glagolev, M., Kleptsova, I., Filippov, I., Maksyutov, S., and Machida, T.: Regional methane emission from West Siberia mire landscapes, *Environ. Res. Lett.*, 6, 045214, 10.1088/1748-9326/6/4/045214, 2011.
- Golovatskaya, E. A., and Dyukarev, E. A.: Carbon budget of oligotrophic mire sites in the Southern Taiga of Western Siberia, *Plant and Soil*, 315, 19-34, 10.1007/s11104-008-9842-7, 2008.
- Granberg, G., Grip, H., Löfvenius, M. O., Sundh, I., Svensson, B. H., and Nilsson, M.: A simple model for simulation
1280 of water content, soil frost, and soil temperatures in boreal mixed mires, *Water Resour. Res.*, 35, 3771-3782, 10.1029/1999WR900216, 1999.
- Heimann, M., Schulze, E. D., Winderlich, J., Andreae, M., Chi, X., Gerbig, C., Kolle, O., Kübler, K., Lavric, J. V., Mikhailov, E., Panov, A., Park, S., Rödenbeck, C. and Skorochood, A.: The Zotino Tall Tower Observatory (Zotto): Quantifying Large Scale Biogeochemical Changes in Central Siberia. *Nova Acta Leopoldina NF*, 117(399), 51-64,
1285 2014.
- Humphreys, E. R., Lafleur, P. M., Flanagan, L. B., Hedstrom, N., Syed, K. H., Glenn, A. J., and Granger, R.: Summer carbon dioxide and water vapor fluxes across a range of northern peatlands, *J. Geophys. Res.: Biogeosciences*, 111, 10.1029/2005JG000111, 2006.
- Humphreys, E. R., Charron C., Brown, M. and Jones, R.: Two bogs in the Canadian Hudson Bay Lowlands and a
1290 temperate bog reveal similar annual net ecosystem exchange of CO₂, *Arct. Antarct. Alp. Res.* 46, 103-113, 2014.
- IPCC: Supplement to the 2006 IPCC Guidelines for National Greenhouse Gas Inventories: Wetlands, edited by: Hiraishi, T., Krug, T., Tanabe, K., Srivastava, N., Baasansuren, J., Fukuda, M., and Troxler, T. G., IPCC, Switzerland, 2014, 2013.

- 1295 Kasurinen, V., Alfredsen, K., Kolari, P., Mammarella, I., Alekseychik, P., Rinne, J., Vesala, T., Bernier, P., Boike, J.,
Langer, M., Marchesini, L. B., Van Huissteden, K., Dolman, H., Sachs, T., Ohta, T., Varlagin, A., Rocha, A., Arain, A.,
Oechel, W., Lund, M., Grelle, A., Lindroth, A., Black, A., Aurela, M., Laurila, T., Lohila, A., and Berninger, F.: Latent
heat exchange in the boreal and arctic biomes, *Glob. Change Biol.*, 20, 3439-3456, 10.1111/gcb.12640, 2014.
- Kormann, R., and Meixner, F. X.: *Boundary-Layer Meteorology*, 99, 207-224, 10.1023/a:1018991015119, 2001.
- 1300 Korrensalo, A., Hájek, T., Alekseychik, P., Rinne, J., Vesala, T., Mehtätalo, L., Mammarella, I., and Tuittila, E.-S.:
Species-specific temporal variation in photosynthesis as a moderator of peatland carbon sequestration, *Biogeosciences*,
14, 257-269, 2017.
- Kurbatova, J., Arneth, A., Vygodskaya, N. N., Kolle, O., Varlagin, A. V., Milyukova, I. M., Tchepakova, N. M.,
Schulze, E. D., and Lloyd, J.: Comparative ecosystem-atmosphere exchange of energy and mass in a European Russian
and a central Siberian bog I. Interseasonal and interannual variability of energy and latent heat fluxes during the
1305 snowfree period, *Tellus B*, 54, 10.3402/tellusb.v54i5.16683, 2002.
- Lafleur, P. M., Roulet, N. T., Bubier, J. L., Frolking, S., and Moore, T. R.: Interannual variability in the peatland-
atmosphere carbon dioxide exchange at an ombrotrophic bog, *Global Biogeochemical Cy.*, 17,
103610.1029/2002gb001983, 2003.
- Lund, M., Lindroth, A., Christensen, T. and Ström, L.: Annual CO₂ balance of a temperate bog, *Tellus*, 59B, 804-811,
1310 2007.
- Mammarella, I., Launiainen, S., Gronholm, T., Keronen, P., Pumpanen, J., Rannik, U., and Vesala, T.: Relative
Humidity Effect on the High-Frequency Attenuation of Water Vapor Flux Measured by a Closed-Path Eddy Covariance
System, *J. Atmos. Ocean. Tech.*, 26, 1856-1866, 10.1175/2009JTECHA1179.1, 2009.
- Mammarella, I., Peltola, O., Nordbo, A., Järvi, L., and Rannik, Ü.: Quantifying the uncertainty of eddy covariance
1315 fluxes due to the use of different software packages and combinations of processing steps in two contrasting
ecosystems, *Atmos. Meas. Tech.*, 9, 4915-4933, 10.5194/amt-9-4915-2016, 2016.
- Masing, V., Botch, M., and Läänelaid, A.: Mires of the former Soviet Union, *Wetlands Ecol. Manage.*, 18, 397-433,
2010.
- Ochsener, T., Sauer, T., and Horton, R.: Soil heat storage measurements in energy balance studies, *Agron. J.*, 99, 311-
1320 319, 2007.
- Oshkin, I. Y., Wegner, C. E., Luke, C., Glagolev, M. V., Filippov, I. V., Pimenov, N. V., Liesack, W., and Dedysh, S.
N.: Gammaproteobacterial methanotrophs dominate cold methane seeps in floodplains of West Siberian rivers, *Appl.*
Environ. Microbiol., 80, 5944-5954, 10.1128/AEM.01539-14, 2014.
- Peichl, M., Sagerfors, J., Lindroth, A., Buffam, I., Grelle, A., Klemetsson, L., Laudon, H., and Nilsson, M. B.: Energy
1325 exchange and water budget partitioning in a boreal minerogenic mire, *J. Geophys. Res.: Biogeosciences*, 118, 1-13,
10.1029/2012JG002073, 2013.
- Price, J. S., Heathwaite, A. L., and Baird, A. J.: Hydrological processes in abandoned and restored peatlands: An
overview of management approaches, *Wetlands Ecol. and Manage.*, 11, 65-83, 10.1023/a:1022046409485, 2003.
- Reichstein, M., Papale, D., Valentini, R., Aubinet, M., Bernhofer, C., Knohl, A., Laurila, T., Lindroth, A., Moors, E.,
1330 Pilegaard, K., and Seufert, G.: Determinants of terrestrial ecosystem carbon balance inferred from European eddy
covariance flux sites, *Geophys. Res. Lett.*, 34, L01402, 10.1029/2006gl027880, 2007.
- Roulet, N. T., Lafleur, P. M., Richard, P. J. H., Moore, T. R., Humphreys, E. R., and Bubier, J.: Contemporary carbon
balance and late holocene carbon accumulation in a northern peatland, *Global Change Biology*, 13(2), 397-411, 2007.

- 1335 Runkle, B. R. K., Wille, C., Gažovič, M., Wilmking, M., and Kutzbach, L.: The surface energy balance and its drivers in a boreal peatland fen of northwestern Russia, *J. Hydrol.*, 511, 359-373, <http://dx.doi.org/10.1016/j.jhydrol.2014.01.056>, 2014.
- Sabrekov, A., Kleptsova, I., Glagolev, M., Maksyutov, S. S., and Machida, T.: Methane emission from middle taiga oligotrophic hollows of Western Siberia, *Tomsk State Pedagogical University Bulletin*, 107, 2011.
- 1340 Sabrekov, A. F., Glagolev, M. V., Kleptsova, I. E., Machida, T., and Maksyutov, S. S.: Methane emission from mires of the West Siberian taiga, *Eurasian Soil Sci.*, 46, 1182-1193, 10.1134/s1064229314010098, 2013.
- Schneider, J., Kutzbach, L., and Wilmking, M.: Carbon dioxide exchange fluxes of a boreal peatland over a complete growing season, Komi Republic, NW Russia, *Biogeochemistry*, 111, 485-513, 10.1007/s10533-011-9684-x, 2011.
- Shimoyama, K., Hiyama, T., Fukushima, Y., and Inoue, G.: Seasonal and interannual variation in water vapor and heat fluxes in a West Siberian continental bog, *J. Geophys. Res.-Atmospheres*, 108, 4648, 10.1029/2003jd003485, 2003.
- 1345 Shulze, E.-D., Lapshina, E., Filippov, I., Kuhlmann, I., and Mollicone, D.: Carbon dynamics in boreal peatlands of the Yenisey region, western Siberia, *Biogeosciences*, 12, 7057-7070, 2015.
- Stepanova, V. A., and Pokrovsky, O. S.: Macroelement composition of raised bogs peat in the middle taiga of Western Siberia (the bog complex Mukhrino) (In Russian) (Макроэлементный состав торфа выпуклых верховых болот средней тайги Западной Сибири (на примере болотного комплекса «Мухрино»)), *Tomsk State University Journal*, 1350 352, 211-214, 2011.
- Stoy, P. C., Mauder, M., Foken, T., Marcolla, B., Boegh, E., Ibrom, A., Arain, M. A., Arneth, A., Aurela, M., Bernhofer, C., Cescatti, A., Dellwik, E., Duce, P., Gianelle, D., van Gorsel, E., Kiely, G., Knohl, A., Margolis, H., McCaughey, H., Merbold, L., Montagnani, L., Papale, D., Reichstein, M., Saunders, M., Serrano-Ortiz, P., Sottocornola, M., Spano, D., Vaccari, F., and Varlagin, A.: A data-driven analysis of energy balance closure across 1355 FLUXNET research sites: The role of landscape scale heterogeneity, *Agr. Forest Meteorol.*, 171-172, 137-152, <http://dx.doi.org/10.1016/j.agrformet.2012.11.004>, 2013.
- Szajdak, L. W., Lapshina, E. D., Gaca, W., Styła, K., Meysner, T., Szczepanski, M., and Zarov, E. A.: Physical, chemical and biochemical properties of Western Siberia Sphagnum and Carex peat soils, *Environ. Dyn. Glob. Clim. Change*, 7, 13-25, 2016.
- 1360 Terentieva, I., Glagolev, M., Lapshina, E., Sabrekov, A., and Maksyutov, S.: High resolution wetland mapping in West Siberian taiga zone for methane emission inventory, *Biogeosciences*, 13, 4615-4626, 2015.
- Turunen, J., Tahvanainen, T., Tolonen, K., and Pitkänen, A.: Carbon accumulation in West Siberian mires, Russia Sphagnum peatland distribution in North America and Eurasia during the past 21,000 years, *Glob. Biogeochemical Cy.*, 15, 285-296, 2001.
- 1365 van Dijk, A., Moene, A. F., and de Bruin, A. R.: The principles of surface flux physics: Theory, practice and description of the ECPack library., *Meteorology and Air Quality Group, Wageningen University, Wageningen, The Netherlands*, 99, 2004.
- Webb, E. K., Pearman, G. I., and Leuning, R.: Correction of Flux Measurements for Density Effects due to Heat and Water-Vapor Transfer, *Q. J. Roy. Meteor. Soc.*, 106, 85-100, 1980.
- 1370 Weiss, R., Alm, J., Laiho, R., and Laine, J.: Modeling moisture retention in peat soils, *Soil Sci. Soc. Am. J.*, 62, 305-313, 1998.
- Vickers, D., and Mahrt, L.: Quality Control and Flux Sampling Problems for Tower and Aircraft Data, *J. Atmos. Ocean. Tech.*, 14, 512-526, 10.1175/1520-0426(1997)014<0512:qcafsp>2.0.co;2, 1997.

- 1375 Wu, J., Kutzbach, L., Jager, D., Wille, C., and Wilmking, M.: Evapotranspiration dynamics in a boreal peatland and its impact on the water and energy balance, *J. Geophys. Res.: Biogeosciences*, 115, 10.1029/2009JG001075, 2010.
- Yu, Z. C.: Northern peatland carbon stocks and dynamics: a review, *Biogeosciences*, 9, 4071-4085, 10.5194/bg-9-4071-2012, 2012.
- 1380 Yurova, A., Wolf, A., Sagerfors, J., and Nilsson, M.: Variations in net ecosystem exchange of carbon dioxide in a boreal mire: Modeling mechanisms linked to water table position, *J. Geophys. Res.: Biogeosciences*, 112, 10.1029/2006JG000342, 2007.